Research Article
Geochemistry, Geophysics, Geosystems
DOI 10.1002/2015GC005885

Supercontinental Inheritance and its Influence on Supercontinental Breakup: The Central Atlantic Magmatic Province and the Break-up of Pangea

Lisa Whalen[1], Esteban Gazel[1*], Christopher Vidito[2], John Puffer[4], Michael Bizimis[3], William Henika[1], Mark J. Caddick[1]

1. *Department of Geosciences, Virginia Tech, Blacksburg, VA 24061, USA*
2. *Earth and Planetary Sciences, Rutgers University, Piscataway, NJ 08854, USA*
3. *Department of Earth and Ocean Sciences, University of South Carolina, Columbia, SC 29208, USA*
4. *Department of Earth and Environmental Sciences, Rutgers University, Newark, NJ 07102, USA*

*corresponding author: egazel@vt.edu

This article has been accepted for publication and undergone full peer review but has not been through the copyediting, typesetting, pagination and proofreading process which may lead to differences between this version and the Version of Record. Please cite this article as doi: 10.1002/2015GC005885

Received: Apr 29, 2015; Revised: Aug 19, 2015; Accepted: Aug 31, 2015

Word count (Abstract 237/Text 9409)

Abstract

The Central Atlantic Magmatic Province (CAMP) is the large igneous province (LIP) that coincides with the breakup of the supercontinent Pangea. Major and trace element data, Sr-Nd-Pb radiogenic isotopes, and high-precision olivine chemistry were collected on primitive CAMP dikes from Virginia (VA). These new samples were used in conjunction with a global CAMP dataset to elucidate different mechanisms for supercontinent breakup and LIP formation. In the Eastern North America Margin, CAMP flows are found primarily in rift basins that can be divided into northern or southern groups based on different tectonic evolution, rifting histories, and supercontinental inheritance. Geochemical signatures of CAMP suggest an upper mantle source modified by subduction processes. We propose that the greater number of accretionary events or metasomatism by sediment melts as opposed to fluids on the northern versus the southern Laurentian margin during the formation of Pangea led to different subduction-related signatures in the mantle source of the northern versus southern CAMP lavas. CAMP samples have elevated Ni and low Ca in olivine phenocrysts indicating a significant pyroxenite component in the source, interpreted here as a result from subduction metasomatism. Different collisional styles during the Alleghanian orogeny in the North and South may have led to the diachroneity of the rifting of Pangea. Furthermore, due to a low angle of

subduction, the Rheic plate may have underplated the lithosphere, then delaminated thus triggering both the breakup of Pangea and the formation of CAMP.

1. Introduction

Wilson cycles, or the formation and breakup of supercontinents are an integral part of plate tectonics [*Wilson*, 1965, 1966]. However, the mechanism or trigger to initiate the breakup of the continental lithosphere is a fundamental missing piece of this unifying theory. Although large igneous province (LIP) formation has been linked to supercontinent breakup [*Storey*, 1995; *Courtillot et al.*, 1999], the formation mechanisms of LIPs are still debated [*King and Anderson*, 1995; *Lustrino*, 2005; *Campbell*, 2007]. Nevertheless, some of the most significant mass extinction events in Earth's history correlate with LIPs [*Courtillot and Renne*, 2003] making LIP formation important not only for understanding mantle dynamics, but also for elucidating relationships between geological and biological processes during the evolution of our planet.

1.1 The Central Atlantic Magmatic Province

The Central Atlantic Magmatic Province (CAMP, Fig. 1) is the LIP temporally related to the breakup of Pangea ~200 Ma [*Marzoli et al.*, 1999; *Blackburn et al.*, 2013] and is one of the largest LIPs in the geologic record, with a volume of 2.3 x 10^5 km^3 and a surficial area of 10^7 km^2 [*McHone*, 2003]. Thus understanding the formation mechanism of CAMP can provide explanations for the formation of LIPs that share similar characteristics. Assessing the role of CAMP in the breakup of Pangea can also help to elucidate the triggering mechanism responsible for the breakup of supercontinents. Some models for CAMP suggest that it may have formed from the impingement of a mantle plume on the lithosphere [e.g. *May,* 1971; *Morgan,* 1983; *Anderson, 1982; White and McKenzie*, 1989; *Hill*, 1991; *Wilson*, 1997; *Courtillot et al.,* 1999; *Ernst and Buchan,* 2002; *Fokin*, 2003]. In this scenario, a hot mantle upwelling impacts the lithosphere, where the plume head undergoes decompression, melts, and emplaces the LIP [e.g. *White and McKenzie*, 1989; *Wilson*, 1997]. This mechanism is problematic for CAMP because no active hot spot or hot spot trail can be linked to the province, nor are there clear geochemical signatures to indicate plume activity or excess mantle potential temperatures [*McHone*, 2000; *Puffer*, 2001; *Herzberg and Gazel,* 2009]. Thus, alternative explanations such as edge-driven convection (EDC) [*King and Anderson*, 1995] has been proposed for CAMP initiation [*McHone*, 2000; *Deckart et al.*, 2005; *Merle et al.*, 2011].

EDC relies on the difference in thickness between the thinner edge of the continent and the thicker interior forming a temperature gradient that drives small-scale convection cells [*King and Anderson*, 1995]. Delamination is another shallow formation mechanism that has been proposed for some continental LIPs [*Lustrino*, 2005]. Delamination occurs when denser lower crust, lithospheric mantle, or underplated material separates or breaks away as either a planar feature or a Rayleigh-Taylor instability and sinks into the asthenospheric mantle. [*Bird*, 1979; *Houseman et al.,* 1981; *Conrad and Molnar*, 1997; *Houseman and Molnar*, 1997; *Kay and Kay*, 1993; *Schott and Schmeling*, 1998]. The resulting influx of hot asthenosphere will melt due to decompression producing uplift, extension, and rifting [*Bird*, 1979; *Houseman et al.,* 1981; *Conrad and Molnar*, 1997; *Houseman and Molnar*, 1997; *Kay and Kay*, 1993; *Schott and Schmeling*, 1998].

This study provides a viable formation mechanism for CAMP that explains the large volume of melt produced, the relatively cool mantle potential temperatures, temporal and chemical evolution, as well as relationship of this LIP to the breakup of Pangea. Despite the large amount of data available for some parts of CAMP there is limited data available for CAMP in Virginia. Therefore, diabase dikes were sampled from different locations around the Danville Triassic rift basin and in the Shenandoah Valley in southwest Virginia (GPS locations in Table S1). This study included our new data in a more complete dataset to address the formation mechanism of CAMP and its relationship to both the assembly and the breakup of Pangea. Additionally, our new data from Virginia was used to assess the source components of CAMP using a high-precision olivine chemistry [*Sobolev et al.*, 2007] never applied to the LIP before.

2. Previous Work

Any attempt at assessing how Pangea broke up must examine if any of the inherited structures and/or chemical signatures from the breakup of the previous supercontinent, Rodinia, or protracted subduction leading to the formation of Pangea played a role. While previous authors [*Schlische et al.*, 2003; *Hatcher*, 2010; *Hibbard et al.*, 2010] have made huge strides towards a large scale, integrated view of the breakup of Pangea, we combined their conclusions with some relatively new relevant geophysical results [*Benoit et al.*, 2014] and the results from our characterization of the source composition from CAMP samples in Virginia, allowing for a new look at the formation mechanism for CAMP and the breakup of Pangea.

2.1 Formation of Pangea: Differences in the Northern and Southern Appalachians

The Paleozoic Appalachian orogeny records the multi-stage, accretion of the most recent supercontinent, Pangea [*Hatcher*, 2010]. After the Middle Ordovician-age Taconic orogeny [e.g. *Hibbard et al.*, 2007; *van Staal et al.*, 2009; *Hatcher*, 2010; *Hibbard et al.*, 2010] these events are not evenly distributed across the Laurentian margin, and thus *Hibbard et al.* [2010] suggested the use of the New York promontory as the division between the northern and southern Appalachians. During the Late Ordovician through the Early Devonian the northern margin records the accretion of Ganderia and Avalonia while the southern margin records the accretion of Carolina [*van Staal et al.*, 2009; *Hibbard et al.*, 2010]. The terminal step in the formation of Pangea was the Alleghanian orogeny that occurred during the Carboniferous period when Gondwana collided obliquely with the northern portion of the Laurentian margin, then rotated clockwise eventually resulting in a head-on collision between Gondwana and the southern portion of the Appalachians. This resulted in the accretion of Meguma in the North and the Suwannee terrane in the South [*Hatcher,* 2002].

2.2 Timing and Age Progression of CAMP Magmatism

Recent work by *Blackburn et al.* [2013] using high-precision U-Pb geochronology on zircons from CAMP basalts definitively linked CAMP with the End Triassic Extinction as well as constrained the beginning of CAMP to the North as opposed to the South as previously thought [*Wilson*, 1997; *Schlische et al.*, 2003]. Furthermore, CAMP lavas decrease in age from North to South. High-titanium quartz normative lavas represent the first pulse of CAMP magmatism with an age of 201.566 ± 0.031 (North Mt. Basalt, Fundy, Nova Scotia) [*Blackburn et al.*, 2013]. Olivine normative lavas, found mostly in the South, are the youngest pulse and have an age of 200.916 ± 0.064 (Butner intrusive, Deep River Basin, North Carolina) [*Blackburn et al.*, 2013]. The rifting of Pangea proceeded in the opposite direction to CAMP magmatism, beginning first in the South [*Schlische et al.*, 2003].

2.3 Breakup of Pangea and CAMP Emplacement: Differences Between the Northern and Southern Appalachians

A series of fault-bounded rift basins related to the initial rifting of Pangea exist along the eastern margin of North America and the western margin of Africa [*Olsen*, 1997]. Significant differences between the basin history of the northern versus the southern Appalachians are evident through a comparison of the timing of sediment deposition between rift basins (Fig. 2) [*Olsen*, 1997; *Schlische et al.*, 2003]. In general, rifting began in the South and ended prior to the emplacement of CAMP basalts, depositing only Triassic-age strata [*Schlische et al.*, 2003]. In the North most

CAMP flows thicken toward the upper border faults of rift basins indicating that they are late synrift flows [e.g. *Olsen et al.*, 1989; *Withjack et al.*, 1995]. Strata in the northern basins span the Triassic and Early Jurassic [*Olsen et al.*, 1989; *Olsen*, 1997] with accelerated rates of sedimentation in the Jurassic [*Olsen et al.*, 1989; *Schlische and Olsen*, 1990].

2.4 Supercontinental Inheritance from Rodinia

Rodinia, the supercontinent preceding Pangea, formed during the Grenville orogeny (1.2 - 0.9 Ga) [*Hatcher*, 2010] and broke up over a 200 myr timespan, during which rifting occurred along what would become the eastern Laurentian margin [*McClellan and Gazel*, 2014]. Supercontinental inheritance, that is the geologic history of a previous supercontinent directing the evolution of its successor, is seen in the rifting history of the Newark, Gettysburg, Culpepper and Barboursville basins (Figs. 1, 2). Similarities between these basins has led to the suggestion that they represent one continuous basin [*Faill*, 2003] and collectively share specific traits with both the northern and southern rift basins. Like the southern basins, deposition in the Newark, Gettysburg, and Culpepper basins began in the Late Triassic, but in common with the northern basins they also contain Jurassic-age strata and synrift CAMP flows [*Olsen*, 1997].

These basins are located adjacent to the Pennsylvania salient, where the central Appalachian Mountains undergo a drastic change in strike [e.g. *Lefort and Van der Voo*, 1981; *Wise*, 2004; *Ong et al.*, 2007]. *Hibbard et al.* [2010] suggested that the New York promontory, which separates first order distinctions between the two portions of the Appalachian orogen, might reflect an inherited structure related to the Neoproterozoic rifting of Rodinia. A failed Neoproterozoic rift was recently imaged adjacent to the Pennsylvania salient using wide-angle reflection and temporary broadband seismic data [*Benoit et al.*, 2014]. The Scranton Rift is buried in the subsurface and, based on adjacent fold and fault geometry, may have acted as a collisional "backstop" during the Alleghanian accretionary event, effectively shaping the Appalachian orogeny [*Benoit et al.*, 2014].

This Rodinia-related relic rift and associated underplated dense material were probably responsible for the change from oblique collision in the North to rotation and eventual head-on collision in the South during the Alleghanian orogeny. Furthermore, we propose that the transitional nature of the Newark, Gettysburg, and Culpepper basin histories [*Schlische et al.*, 2003] are also due to this subsurface inherited feature, which acted as a rigid "buffer" and effectively negated much of the uplift, which may have affected the northern and southern Appalachians throughout the Mesozoic [*Frizon de Lamotte et al.,* 2015]. In this study we use the Scranton Rift to separate northern CAMP (located to the north of the Scranton rift) [*Dostal and Durning*, 1998; *Marzoli et al.*, 2011; *Merle et al.*, 2013], southern CAMP (located to the south of the Scranton rift [*Callegaro et al.*, 2013; *Mazza et al.*, 2014] and transitional CAMP (located within or nearby the Newark, Gettysburg, and Culpepper basins) [*Marzoli et al.*, 2011; *Merle et al.*, 2013].

2. Materials and Methods

Sample SPG-111 was selected for $^{40}Ar/^{39}Ar$ geochronology because it contained ample biotite, an ideal mineral to date with this method. Incremental step heating was performed at the New Mexico Geochronology Research Laboratory (see supplementary materials for details). Samples were analyzed for major and trace elements at the GeoAnalytical Lab at Washington State University. Major elements were collected by x-ray fluorescence (XRF) on a ThermoARL XRF, while trace elements were collected by an Agilent model 4500 ICP-MS. Data from two additional samples (042 Singers Glen and 12DJ Mosque 1) are from *Mazza et al.* [2014]. Analyses of Sr, Nd, and Pb radiogenic isotope ratios were carried out at the Center for Elemental Mass Spectrometry, University of South Carolina following established techniques for this lab [e.g *Bizimis et al*., 2013; *Khanna et al*., 2014]. Using a modified version of the high precision method of *Sobolev et al.* [2007] 71 olivine phenocrysts were analyzed from 7 different dikes in Virginia using only the most primitive (in olivine control) basalts. Major and trace element data for CAMP olivine phenocrysts were collected at Rutgers University on a JEOL JXA-8200 Superprobe. Analytical protocols and additional details are available in the Supplementary Materials.

Our new data was incorporated into the geochemical dataset from the literature from CAMP dikes and flows collected in Africa, Europe, and North and South America (Fig. 1) [*Bertrand*, 1991; *Dostal and Durning*, 1998; *Puffer and Volkert*, 2001; *Cebriá et al.*, 2003; *Jourdan et al.*, 2003; *Marzoli et al.*, 2004; *Deckart et al.*, 2005; *Verati et al.*, 2005; *Mahmoudi and Bertrand*, 2007; *Martins et al.*, 2008;

Marzoli et al., 2011; *Merle et al.*, 2011; *Callegaro et al.*, 2013; *Merle et al.*, 2013; *Callegaro et al.*, 2014; *Mazza et al.*, 2014]. We also compiled available radiogenic isotope data for the Costal New England Magmatic Province (CNE) that overlaps with the onset of CAMP [*McHone and Butler*, 1984; *McHone*, 1992; *Pe-Piper et al.*, 1992; *Pe-Piper and Reynolds*, 2000] and for the accreted terrenes where CAMP was emplaced [*Pettingill et al.*, 1984; *Sinha et al.*, 1996; *Currie et al.*, 1998; *Pe-Piper and Piper*, 1998].

3. Results

A single $^{40}Ar/^{39}Ar$ age was obtained for SPG111, making this the first CAMP sample dated in southwest Virginia (Table S1). After evaluating the mean calculated age of 202.81±0.55 Ma with the inverse isochron technique, the calculated age was 201±2 Ma (Fig. S1). This confirms the connection of this dike with the CAMP event of 201.566 ± 0.031 Ma [*Blackburn et al.*, 2013].

New major and trace element data are reported in Table S1. Following nomenclature originally defined for CAMP lavas [*Weigand and Ragland*, 1970], the samples analyzed consist of low-Ti tholeiites: olivine normative and quartz normative basalts, which we will call here low-Ti basalts and basaltic andesites respectively. The low-Ti basalt samples have primitive Mg#s ([molar MgO/FeO+MgO]*100) ranging from 64.7 to 72.5%. SiO_2, CaO and Al_2O_3 decrease with increasing MgO, with the opposite occurring for NiO, suggesting that olivine was the main fractionating phase. A primary magma was calculated from the most primitive low-Ti basalt sample SPY681 (that required <10% olivine addition). Liquid lines of descent (LLDs) were modeled for CAMP low-Ti basalts using the software, Petrolog3 [*Danyushevsky and Plechov*, 2011] showing that they are in olivine control (Fig. S2A-C, Supplementary Materials). The low-Ti basaltic andesites Mg#s range from 42 to 53%. CaO decreases with decreasing MgO, while K_2O increases and Al_2O_3 remains relatively unchanged suggesting a cotectic crystallization of olivine and clinopyroxene (Fig. S2), followed by other phases (e.g, plagioclase) as fractionation proceeded. The same primary starting composition used for the Petrolog3 LLD models was too low in silica to replicate the trends of the low-Ti basaltic andesites. Primary magmas of varying degrees of enrichment in silica were estimated and then modeled in Petrolog3. A primary magma with 50.0 wt.% SiO_2 and 0.5 -1.0 wt.% H_20 replicated the low-Ti basaltic andesite trends the best (Fig. S2G-I).

Our new CAMP samples, plotted in a primitive mantle normalized multi-element diagram [*McDonough and Sun,* 1995] (Fig. 3) show relative high field strength element (e.g. Nb, Ta and Ti) depletions as well as large-ion lithophile element (LILE) enrichments. As expected, the low-Ti basaltic andesites are more enriched in trace elements relative to the basalts as a result of fractional crystallization discussed above.

Measured radiogenic isotope ratios, associated errors, and age-corrected isotope ratios (corrected to 200 Ma) are reported in Table S1. Age corrected isotope ratios are plotted in Fig. 3. The basalts have lower $^{143}Nd/^{144}Nd_{200Ma}$ (0.51221 -

0.51234), $^{206}Pb/^{204}Pb_{200Ma}$ (18.27 - 18.37), $^{207}Pb/^{204}Pb_{200Ma}$ (15.60 - 15.63), $^{208}Pb/^{204}Pb_{200Ma}$ (38.21 - 38.27) and higher $^{87}Sr/^{86}Sr_{200Ma}$ ratios (0.70587 - 0.71075) than the basaltic andesites, which have $^{143}Nd/^{144}Nd_{200Ma}$: 0.51230 - 0.51243; $^{206}Pb/^{204}Pb_{200Ma}$: 18.52- 18.65; $^{207}Pb/^{204}Pb_{200Ma}$: 15.60- 15.64; $^{208}Pb/^{204}Pb_{200Ma}$: 38.20- 38.44; $^{87}Sr/^{86}Sr_{200Ma}$: 0.70489 - 0.70625. Both the low-Ti basalts and basaltic andesites from Virginia, sampled for this study plot in the range of published southern CAMP [*Callegaro et al.,* 2013; *Mazza et al*., 2014] except for one basalt (sample PHT911, Table S1), which has a high $^{87}Sr/^{86}Sr_{200Ma}$ value of 0.71075. Sample BLR531B, a low-Ti basaltic andesite increases the range of $^{206}Pb/^{204}Pb_{200Ma}$ for southern CAMP to 18.65. Sample STS971, also a low-Ti basaltic andesite is a radiogenic endmember for southern CAMP as it has a $^{207}Pb/^{204}Pb_{200Ma}$ value of 15.64, and a $^{208}Pb/^{204}Pb_{200Ma}$ value of 38.44.

New high-precision major and trace element data from olivine phenocrysts (Table S2; Fig. 5) show elevated Ni and Fe/Mn as well as low Ca and Mn relative to the values expected for peridotite derivative magmas [*Sobolev et al.*, 2007; *Qin and Humayun*, 2008; *Herzberg*, 2010; *Foley et al.*, 2013].

4. Discussion

4.1. Trace Element Signatures of CAMP Magmas

CAMP samples from Virginia analyzed for this study are similar to CAMP samples from the literature from all along the Eastern North American margin

[*Dostal and Durning*, 1998; *Puffer and Volkert*, 2001; *Marzoli et al.*, 2011; *Callegaro et al.*, 2013; *Merle et al.*, 2013; *Mazza et al.*, 2014] in that they display large-ion lithophile element (LILE) (e.g. Ba, Pb, K, Fig. 3) and light rare earth element (LREE) enrichments and high-field strength element (HFSE) (e.g. Nb and Ta, Fig. 3) depletions typical of arc magmas. Elevated LREE/heavy rare earth element (HREE) ratios alone do not necessarily imply a subduction-modified source, but taken together with low HFSE contents and no significant differences in melt fraction, enrichment in LREE compared to HREE can be used as evidence of mantle metasomatism in subduction systems [*Pearce and Peate*, 1995]. This signature suggests, in accordance with *Puffer* [2001] that from a geochemical perspective CAMP lavas are broadly more arc-like than plume-like.

Subduction-sensitive Th/Yb, and fluid-immobile Nb/Yb element ratios are particularly useful for distinguishing between subduction and mantle plume influenced environments. In Figure 6A these element ratios from CAMP samples are compared to the mantle array as defined by global mid-ocean ridge basalt (MORB) and intraplate ocean island basalt (OIB) data. Like lavas from the Lesser Antilles, Marianas and Cascades arcs, most CAMP lavas (including the new samples from Virginia) plot above the mantle array suggesting a subduction-modified source. We divide CAMP terranes (Fig. 1) into northern, southern and transitional groups based on their location with respect to the Scranton Rift. Southern CAMP lavas plot nearest to or within the mantle array indicating less of a subduction component in the South. High Th/Yb and Nb/Yb ratios of transitional and northern CAMP suggest mixing between relatively depleted and enriched arc-modified sources. Ce/Yb ratios of CAMP lavas show an increase in Ce/Yb from South to transitional to North (Fig. 6B). In terms of Nb/U, another trace element ratio that is indicative of source compositions, northern and transitional CAMP have lower values than southern CAMP samples (Fig. 6B) placing them in the same Nb/U space as lavas from an arc-modified source (Nb/U < 20) [*Hofmann et al.*, 1986; *Hofmann*, 2007]. Southern CAMP spans the entire range of Nb/U ratios including those derived from non-subduction modified sources such as MORB and OIB [*Hofmann et al.*, 1986; *Hofmann*, 2007]. Most of the new samples from Virginia plot within the bounds of published southern CAMP [*Callegaro et al.*, 2013], with the exception of a few low-Ti basaltic andesites that plot at slightly higher Th/Yb and Nb/Yb ratios suggesting a stronger subduction influence for these samples. The low-Ti basalts collected in Virginia for this study plot within the confines of published southern CAMP data, with the low-Ti basaltic andesites plotting as the high Ce/Yb endmember of southern CAMP.

4.2 Sr-Nd-Pb Radiogenic Isotope Signatures of CAMP Magmas

We age-corrected Sr-Nd-Pb radiogenic isotopic ratios to 200 Ma for our new data reported in Table S1 as well as for northern, transitional and southern CAMP, and for CAMP sampled in Africa, Europe and South America. Additionally we included Sr-Nd-Pb radiogenic isotope ratios for the accreted terranes of Avalonia [*Pe-Piper and Piper*, 1998], Meguma [*Currie et al.*, 1998] and Carolina [*Pettingill et al.*, 1984; *Sinha et al.*, 1996]. We also included data from the Coastal New England magmatic province (CNE) [*McHone and Butler*, 1984; *McHone*, 1992; *Pe-Piper et al.*, 1992; *Pe-Piper and Reynolds*, 2000], because its age range (255 - 202 Ma) broadly overlaps with the onset of CAMP magmatism at ~200 Ma.

Northern and transitional CAMP lavas have higher $^{143}Nd/^{144}Nd_{200Ma}$ and Pb isotopic ratios while southern CAMP covers a wider range for both $^{87}Sr/^{86}Sr_{200Ma}$ ratios, $^{143}Nd/^{144}Nd_{200Ma}$ and Pb isotopic ratios (Fig. 4A-C). (Fig. 4A). CAMP lavas plot in a mixing line between depleted MORB mantle (DMM), and an enriched source and to some extent HIMU (high μ = $^{238}U/^{204}Pb$) (Fig. 4B,C). South American CAMP also plots towards a HIMU component along with the Coastal New England lavas on a $^{87}Sr/^{86}Sr_{200Ma}$ - $^{143}Nd/^{144}Nd_{200Ma}$ diagram (Fig. 4A) however these high-Ti tholeiites may represent a younger pulse of CAMP magmatism recording the transition to oceanic crust [*Deckart et al.*, 2005].

In $^{143}Nd/^{144}Nd_{200Ma}$ - $^{206}Pb/^{204}Pb_{200Ma}$, as well as in Pb isotope space, northern and transitional CAMP plot alongside the Meguma and Avalonia terranes (Fig. 7), while the Carolina terrane plots closer to southern CAMP. Erosion of the Avalonia, Meguma and Carolina terranes prior to accretion could have led to sediment input during subduction, which would then be incorporated into the upper mantle through the input of sediment melts with the overlying mantle wedge beneath Laurentia, accounting for the Nd and Pb isotopic composition of the northern and transitional CAMP lavas [*Merle et al.*, 2013].

For northern and transitional CAMP this is evidence that the source of these magmas inherited their enriched continental-like trace element and radiogenic isotope composition from subduction-related processes as opposed to crustal contamination, which has been shown to represent a minimal contribution for any of the CAMP terranes [*Puffer*, 2001; *Merle et al.*, 2011; *Callegaro et al.*, 2013; *Callegaro et al.*, 2014]. The low $^{187}Os/^{188}Os$ ratios of CAMP samples argue against significant crustal contamination processes in the generation of this LIP [*Merle et al.*, 2011; *Callegaro et al.*, 2013].

Furthermore, assimilation-fractional-crystallization (AFC) calculations modeling an Atlantic plume [*Holm et al.,* 2005] or MORB [*Gale et al.,* 2013] starting composition that was then contaminated with local Blue Ridge basement (Fig. S3). The AFC models were unsuccessful in replicating trace element and Sr-Nd-Pb compositions of the low-Ti basalts and basaltic andesites analyzed in this study (see details in supplementary materials). AFC models by *Merle et al.* [2013] using both a plume and a MORB starting composition also argue against crustal contamination as the models require an unrealistic amount (up to 35%) of assimilation to get close to the radiogenic isotopes of CAMP samples while keeping primitive mantle-derived major element compositions. On the other hand, calculations to reproduce northern CAMP lavas required only ~3-5% sediment [*Merle et al.*, 2013], which is within the range (2-6%) of the sediment budget of arc lavas [*Plank*, 2005].

As a current example of this process the Lesser Antilles highly radiogenic isotope signature has been attributed to sediment derived from the South American cratonic basement and transported by the Orinoco River [e.g. *White and Dupré*, 1986] with the Lesser Antilles basalts requiring a sediment component of up to 10% [*Carpentier et al.*, 2008]. Transport of eroding sediment via rivers into the subduction trench, as well as by deep underwater currents may account for southern CAMP's isotopic range from the less evolved Carolina through Meguma and Avalonia, or sediment may have played less of a role in the metasomatization of the mantle beneath the southern margin of Laurentia.

4.3 Discriminating between Metasomatism by Fluids or Sediment-melt Components in CAMP Magmas

Merle et al. [2013] showed that northern and transitional CAMP were influenced by sediments or sediment melts based on LREE and Th/Yb coupled with initial Nd-isotopes [*Woodhead et al.,* 2001]. On a Ba/La-Th/Yb diagram (Fig. 9A), northern and transitional CAMP plot along the increasing Th/Yb trend observed for several arcs, which has been interpreted as incorporation of a sediment component [e.g. *Class et al.,* 2000]. Northern and transitional CAMP also have higher middle rare earth element (MREE) contents relative to heavy rare earth elements (HREE) than southern CAMP as expressed by lower Dy/Dy* ($Dy/Dy^* = Dy_N/(La_N)^{4/13}*(Yb_N)^{9/13}$) (Fig. 9B) and higher Dy/Yb values [*Davidson et al.,* 2013]. Dy/Dy* and Th/Yb correlate with $^{143}Nd/^{144}Nd_{200Ma}$ for northern (R^2 = 0.77, and 0.55 respectively) and transitional (R^2 = 0.91, 0.35 respectively) CAMP (Figs 9C, D). Taken as a group, Th/Yb and Dy/Dy* for northern and transitional CAMP also correlate with $^{143}Nd/^{144}Nd_{200Ma}$ (R^2 = 0.81, 0.55 respectively) (Figs 9C, D). Th/Yb for southern CAMP does not change as Ba/La increases (Fig. 9A) suggesting a limited role for sediment melt input and more of a fluid-dominated influence [*McCulloch and Gamble*, 1991; *Woodhead et al.,* 2001]. There is no correlation between

$^{143}Nd/^{144}Nd_{200Ma}$ and Th/Yb (Fig. 9C) and only a weak correlation between $^{143}Nd/^{144}Nd_{200Ma}$ and Dy/Dy* for southern CAMP (Fig. 9D) (R^2=0.21).

On a Dy/Dy*-Dy/Yb plot, CAMP samples plot similarly to arc samples as they plot along the MORB array of *Davidson et al*. [2013], but offset towards lower Dy/Yb values (Fig. 9B) [*Davidson et al.,* 2013]. *Davidson et al.* [2013] suggested that the negative trend of arc data towards lower Dy/Dy* and higher Dy/Yb values as a possible influence of sediment melts. We suggest that the sediment signature was incorporated into the subcontinental mantle by sediment melts during the Paleozoic subduction that formed Pangea [*Pegram,* 1990; *Puffer*, 2001, 2003; *De Min et al.,* 2003; *Deckart et al*., 2005; *Dorais and Tubrett*, 2008; *Merle et al.,* 2011, 2013; *Murphy et al.,* 2011; *Callegaro et al.,* 2013]. This interpretation is strengthened by the Th/Yb and Ce/Yb trends [*Woodhead et al.,* 2001; *Hawkesworth et al.,* 1993, 1997] as well as strong correlations between Dy/Dy* and $^{143}Nd/^{144}Nd_{200Ma}$ (Fig. 9D) for northern and transitional CAMP.

Northern and transitional CAMP show positive trends between Dy/Dy* and Dy/Yb (Fig. 9B). A subset of mostly southern CAMP (including the Virginia basalt samples analyzed for this study) plot within the lower lefthand corner of the diagram (Dy/Dy* < 1.0, Dy/Yb < 1.55) and also show a positive trend between Dy/Dy* and Dy/Yb. Samples plotting in this corner of the diagram have u-shaped REE patterns, which *Davidson et al*. [2013] suggested indicates amphibole or clinopyroxene fractionation. Nevertheless in our samples there is no correlation between Dy/Dy* and MgO, and some of these samples are in an olivine control trend, indicating instead that these u-shaped REE patterns are a feature inherited from the source. U-shaped REE patterns from mantle xenolith samples (Fig. 9B) have been interpreted as the result of melt-rock reaction [e.g. *Chalot-Prat and Boullier,* 1997; *Lenoir et al.,* 2000; *Zhang et al.,* 2012; *Ackerman et al.,* 2013*; Bénard and Ionov*, 2013] due to melt migration through the mantle wedge [*Navon and Stoper,* 1987; *Ackerman et al.,* 2007, 2013].

4.4 CAMP Source Lithology Composition from High-Precision Olivine Chemistry and Modeled Primary Magmas

Several studies have attempted to include the effects of pressure and temperature in parameterizations of $D_{Ni}^{Ol/L}$ [e.g., Li and Ripley, 2010; *Niu et al.*, 2011; Matzen et al., 2013] with varying degrees of success [*Herzberg*, 2011; *Herzberg et al.*, 2013; 2014], however the *Beattie et al.* [1991] parameterization is only dependent on $D_{MgO}^{Ol/L}$, which effectively accounts for temperature and will be used here. The additional terms used by other studies [e.g., *Li and Ripley*, 2010; *Niu et al.*, 2011; *Matzen et al.,* 2013] to account for pressure and temperature negatively impacted the ability of the parameterization to replicate experimentally derived $D_{Ni}^{Ol/L}$, which may be due to these terms being model-dependent [*Herzberg et al.*, 2013]. The *Beattie et al.* [1991] model has been the most reliable choice for replicating experimentally derived Ni values in olivine as this model produces the lowest root mean square error (RMSE= 1.1) while the temperature dependent model from *Matzen et al.* [2013] yields a RMSE of 2.5 and the pressure dependent (0-3 GPa) model of *Niu et al.* [2011] yields a RMSE of 2.1 [*Herzberg et al.*, 2014]. Ni systematics in olivine phenocrysts have therefore shown to be a viable tool for evaluating source lithology [*Sobolev et al.*, 2005; *Sobolev et al.*, 2007; *Wang and Gaetani,* 2008; *Herzberg*, 2011].

CAMP olivine data collected from basalts in Virginia for this study show elevated Ni and low Ca concentrations relative to peridotite derived olivines indicating a pyroxenite source component for CAMP [Sobolev et al., 2007; Herzberg, 2011]. CAMP olivine phenocrysts systematically plot alongside data from Mauna Kea or at transitional values between data from mid-ocean ridges and Mauna Kea (Fig. 5). The data from Mauna Kea has been interpreted as coming from a second-stage pyroxenite source that formed from the reaction of a high-silica melt from eclogite with peridotite. Ca and Fe/Mn values obtained for olivine phenocrysts from CAMP plot between samples from Mauna Kea and MORB and may indicate both peridotite and pyroxenite source lithologies for CAMP [*Sobolev et al.*, 2005]. Our new data contrast with those published by *Callegaro et al.* [2013], who suggested that it was unlikely that the source of CAMP contained a pyroxenite component based on their analyses of olivine phenocrysts. Our results, which utilize a modified high-precision method from *Sobolev et al.* [2007] (details in the Supplementary Materials) indicate that a pyroxenite component probably contributed significantly to the source of CAMP.

In order to determine which type of pyroxenite was involved, CAMP primary magma compositions (Table S3) were calculated by taking the bulk rock compositions of lavas in olivine control and adding olivine until equilibrium with the maximum forsterite (Fo) content observed in CAMP magmas (Fo_{89} *Callegaro et* *al.*, [2013]) was achieved (using a variable Fe-Mg partition coefficient for olivine – liquid with an initial value of 0.32 [*Roeder and Emslie*, 1970; *Toplis*, 2005]). These primary magma compositions contain 11.5 to 19.8 wt.% MgO, and 46.93 to 52.43 wt.% SiO_2. The modeled results are plotted in the pseudoternary system olivine-calcium Tschermak's (CATS)-pyroxene-quartz projected from diopside [*O'hara*, 1968] (Fig. 8). CAMP primary magmas project onto the high-SiO_2 pyroxenite side of the pyroxene-garnet plane, which acts as a thermal divide [*Kogiso et al.*, 2004]. Source lithologies with excess silica (olivine-free source) can produce primary magmas that plot on the high-SiO_2 side of the diagram [*Herzberg*, 2011]. This suggests that CAMP primary magmas likely melted from a silica-rich, olivine-free pyroxenite source lithology, which could be the result of high-silica melts formed from subducted material (sediment, subducting oceanic crust) that reacted with mantle peridotite, in a process similar to that suggested by *Sobolev et al.* [2005; 2007].

The new olivine data together with trace elements signatures and radiogenic isotopes argue for a significant sediment component in the source of CAMP lavas. As the ratio of silica-rich melt to peridotite increases, the source will change from re-fertilized peridotite to olivine-bearing pyroxenite, and then to an olivine-free pyroxenite. Additionally the Ni and Fe/Mn of olivine phenocrysts crystallizing from the primary melt will also increase, while Ca decreases [*Herzberg et al.*, 2014]. Further supporting the possibility of high-silica pyroxenite the modeled LLD for the basaltic andesites analyzed in the study require a primary magma rich in silica (Fig. S2). Northern and transitional CAMP magmas have on average even higher SiO_2

contents suggesting the possibility of a higher contribution of pyroxenite-derived melt in the source than those from the South, which resulted in more evolved primary magmas no longer in an olivine-control trend.

4.5 Evaluation of Mechanisms for Pangea Break-up and the Generation of CAMP

Mantle plume activity has been suggested as the formation mechanism for LIPs [*White and McKenzie*, 1989], but because the plume model is inconsistent with the formation of CAMP, alternative explanations such as edge-driven convection (EDC) [*King and Anderson*, 1995] have been invoked. However, EDC does not explain the observed differences between northern and southern CAMP. More crustal thickening occurred in the South during the Alleghanian orogeny [*Hatcher*, 2002], which could lead to a greater difference in the thickness between the edge of the continental lithosphere and the orogenic root. A substantial difference in lithospheric thickness can cause a localized convection cell to form in the mantle, which could explain earlier rifting in the southern basins. However, EDC does not explain why rifting was accompanied by synrift magmatism in the North but not in the South as would be expected. Another issue with the EDC model is that *Missenard and Cadoux* [2012] show that EDC cannot persist if plate velocities exceed 1 cm a^{-1}. Absolute plate motions are not available for North America for the Triassic, but *Ruiz-Martínez et al.* [2012] calculated that Pangea was moving at an average speed of 8 cm/year at 200 Ma, using Africa as a fixed reference in order to approximate absolute velocities. This suggests that EDC would not have been viable in the mantle beneath Pangea at the time of rifting.

Continental insulation of the mantle leading to elevated mantle temperatures and magmatism has been suggested as a formation mechanism for CAMP [*Anderson*, 1982; *Verati et al*., 2005; *Coltice et al.,* 2007, 2009; *Herzberg and Gazel*, 2009; *Hole*, 2015]. Although this model is consistent with the reported mantle potential temperatures, it does not explain why rifting is asynchronous with magmatism in the South, nor the age progression of CAMP magmatism. Geodynamic models indicate the magmatism induced by continental insulation would be tectonically controlled [*Coltice et al.*, 2009], but dikes in the South crosscut both pre- and synrift structures indicating that magmatism was not structurally controlled [*Schlische et al.*, 2003].

Delamination could be a formation mechanism for LIPs [*Lustrino*, 2005]. Ductile delamination is controlled by phase changes in the lithosphere resulting in density instabilities as well as low viscosity [*Conrad and Molnar*, 1997; *Houseman and Molnar*, 1997; *Schott et al.*, 2000; *Tanton and Hager*, 2000; *Elkins-Tanton*, 2005]. Delamination may be common during supercontinent formation [*Kay and Kay*, 1993] as it is likely to occur in areas that have undergone crustal shortening [e.g. *Kay and Kay*, 1993; *Schott and Schmeling*, 1998; *Conrad*, 2000; *Morency et al.*, 2002]. The eastern margin of Laurentia experienced subduction related to several collisional events [*Hatcher*, 2010; *Hibbard et al.*, 2010]. Both the orogenic keels formed during these events and the subducting plates themselves are likely candidates for delamination.

Reduced crustal thicknesses at the center of the Appalachian orogenic belt in Newfoundland [*Hall et al.*, 1998] could indicate delamination. A fossil anisotropy indicative of extension perpendicular to the Appalachian orogeny was detected using shear-wave birefringence across the New England region [*Levin et al.*, 2000]. The anisotropy may have resulted from Late Paleozoic delamination and extension [*Levin et al.*, 2000]. Based on the uniformity of the anisotropy layer, it must post-date the Alleghanian orogeny. Therefore the proposed delamination event could be related to the formation of CAMP near the Triassic-Jurassic boundary.

Finally, CAMP is part of the group of continental LIPs with arc geochemical signatures [*Puffer*, 2001]. Similarities between the LIPs with arc affinities and arc magmas may be due to the melting of subduction-metasomatized mantle [*Pegram,* 1990; *Puffer*, 2001, 2003; *De Min et al.,* 2003; *Deckart et al*., 2005; *Dorais and Tubrett*, 2008; *Merle et al.,* 2011, 2013; *Murphy et al.,* 2011; *Callegaro et al.,* 2013]. Subduction-metasomatized lithosphere is also more likely to delaminate due to heating, and hydration which lower its viscosity [*Elkins-Tanton*, 2005] and melt emplacement [*Jull and Kelemen*, 2001] and removal, which can leave behind mafic residues that can lead to density instabilities [*Herzberg et al.*, 1983; *Kay and Kay*, 1993; *Elkins-Tanton*, 2005].

4.6 Proposed Model for the Break-up of Pangea and CAMP

Using the Scranton Rift to demarcate northern, transitional, and southern CAMP groups, the geochemical variation between northern and southern CAMP could be attributed to a difference in the amount of subduction experienced by the northern and southern margins of Laurentia. While the Scranton Rift represents a possible structural and not a chemical control on the lavas themselves this geochemical variation is less obvious, without separating out the CAMP flows preserved in the rift basins along the East coast of North America into groups based on their position relative to the Scranton Rift. If the Scranton Rift did act as a "collisional backstop" causing a rotation in the direction of collision between Gondwana and Laurentia this may have led to a change in the angle of subduction. This could affect the rate of subduction erosion [*Keppie et al*., 2009; *Stern*, 2011] and thus the amount of sediment incorporated into the mantle. Smaller angles of subduction favor subduction erosion of the upper plate [*Keppie et al.,* 2009] and could explain the more prominent sediment signal in northern and transitional CAMP as opposed to southern CAMP.

We propose that differences in the accretionary history of the northern and southern Appalachians (Fig. 10A) can account for the diachroneity in rifting, the chemical differences in CAMP lavas from the North and South, and could be responsible for triggering for the breakup of Pangea. Subduction of the Rheic plate [*Moran et al.*, 2007; *Woodcock et al.*, 2007] at a very low angle (Fig. 10B) may have resulted in the underplating of the slab to the base of the lithosphere beneath Laurentia. During the Alleghanian collisional event, oblique, subduction in the North may have led to a jamming of the subduction zone when the collisional front impacted the Scranton Rift and could no longer advance (Fig. 10B). This blocking of the subduction zone may have led to a rotation of the subduction direction, as seen for example in the subduction of the Hikurangi Plateau beneath New Zealand [*Davy*, 2014], resulting in head-on collision in the South (Fig. 10C).

The head-on collision of Gondwana with the southern portion of Laurentia (Fig. 10C) possibly led to greater overthickening of the crust in the South than in the North. This resulted in a denser orogenic keel surrounded by a less dense asthenospheric mantle and to earlier orogenic collapse and delamination [*Sacks and Secor*, 1990; *Samson et al.*, 1995] as documented by the onset of rifting in the South at ~230 Ma, probably with a similar situation in the Fundy and Argana basins in the North. While the small episodes of earliest rifting in the North were relatively isolated to the Argana and Fundy basins, rifting in the South was widespread at ~230 Ma, but unaccompanied by volcanism. This initial orogenic collapse in the South may have served to heat the upper mantle as hotter material ascended to replace the foundering material permitting magmatism closer to 200 Ma [*Nelson*, 1992]. Additionally the upper mantle beneath Pangea may have been warmer due to continental insulation [*Anderson*, 1982; *Coltice et al.,* 2009; *Herzberg and Gazel*, 2009; *Hole*, 2015].

Subduction of the Rheic plate continued towards the North, where the slab was not constricted by the Scranton Rift, straining and eventually tearing the slab (Fig. 10E). A small tear in a subducting slab can propagate laterally due to slab pull [*Wortel and Spakman*, 2000]. Tectonic events leading to the formation of the Central Range of New Guinea and the Talamanca Range in Central America show that the jamming of a subduction zone can lead to a slab tear, delamination, and magmatism

[*Cloos et al.*, 2005; *Gazel et al.*, 2011]. Potentially, a tear in the Rheic slab could have led to mantle upwelling, which over time heated and destabilized the underplated oceanic slab eventually resulting in delamination, which triggered more rifting in the North. In agreement with geodynamic models of lithospheric delamination, [*Elkins-Tanton*, 2005] approaching the eruption of CAMP and continuing into the Jurassic, there was active subsidence with an increase in the sedimentation rate right at the time of eruption (Fig. 11) [*Olsen*, 1997; *Schlische et al.*, 2003].

Uplift due to mantle upwelling could explain the hiatus in sedimentation in the Fundy basin in Nova Scotia [*Schlische et al.*, 2003] (Fig. 2, and 11) during the Late Triassic (230-215 Ma). Thermal doming has been suggested to explain the Late Triassic unconformity in the CAMP basins in Nova Scotia and Morocco [*Frizon de Lamotte et al.,* 2015]. Late Triassic alkaline Costal New England (CNE) magmatism [*McHone and Butler*, 1984; *McHone*, 1992; *Pe-Piper et al.*, 1992; *Pe-Piper and Reynolds*, 2000] peaks during the hiatus in sedimentation in the Fundy Basin (Fig. 11) and could represent an early stage of rifting or uplift (Fig. 10E) prior to the main phase of rifting [*Ross*, 1992; *Swanson*, 1992] as high-potassium silica-rich magmas preceding mafic, extensionally-related magmas agrees with the delamination model of *Kay and Kay* [1993]. Alternatively CNE lavas may be from the slab tear itself, which acted as a trigger for the delamination event responsible for CAMP through heating of the underplated, now eclogitized slab, reducing its viscosity and increasing the likelihood of delamination (Fig. 10E). The oldest $^{40}Ar/^{39}Ar$ age reported for CNE is 246±4 for a dike in Massachusetts [*Ross,* 2010]. While the youngest $^{40}Ar/^{39}Ar$ ages reported for CNE dikes are in Plymouth, Nova Scotia of

203±15 [*Pe-Piper and Reynolds*, 2000] with the oldest CAMP lava flows located nearby in the Fundy basin, Nova Scotia. We suggest this decrease in age in the CNE dikes from closer to the Scranton Rift toward the site of the onset of CAMP magmatism may indicate the direction of the initial tear in the Rheic slab.

Continued heating due to mantle upwelling through the slab tear eventually led to slab foundering in the North, culminating in the upwelling that led to CAMP magmatism (beginning in the Fundy basin on Laurentia and in the Argana basin in Africa) (Fig.s 1 and 10F). The magmatism was voluminous and extensive due to heating from the upwelling asthenosphere, as well as the presence of a significant pyroxenite component derived from previous subduction events (Fig. 10A). Subduction-related volatiles like H_2O added to the overlying mantle wedge by arc metasomatism helped to reduce the melting temperature [e.g. *Hirschmann et al.*, 1999] increasing the amount of melting achieved at lower temperatures. Melts of the lithosphere that had been metasomatized during past subduction events could be responsible for the arc-like magmas typical of CAMP [*Puffer*, 2001; 2003], as well as the low $^{187}Os/^{188}Os$ combined with enriched Sr-Nd-Pb isotopic ratios [*Callegaro et al.*, 2013; *Merle et al.*, 2013]. Upwelling in the North propagated to the South, where earlier heating may have facilitated melting [*Nelson*, 1992]. This upwelling could have then facilitated the weakening of the remaining slab beneath the southern portion of the margin of Laurentia beginning below the Scranton Rift. Beneath North Carolina the crust is reduced to 46 km compared to the average local crustal thickness of ~50 km [*Hawman*, 2008]. In addition, a fossilized slab located at 90 -100 km has been interpreted as evidence of delamination beneath the Carolina terrane due to eclogitization of the lower crust [*Wagner et al.*, 2012]. The west dipping fossilized slab [*Wagner et al.*, 2012] could be the remains of the Rheic slab that underplated the Laurentian lithosphere during the Alleghanian orogeny.

5. Conclusions

The northern Appalachians are the product of at least four different orogenic events terminating with the accretion of Ganderia, Avalonia and Megmua, while the southern Appalachians resulted from the accretion of Carolina, and Suwannee terranes. The difference in the number and size of accretionary events is consistent with an increase in arc-modification of the mantle beneath Laurentia. Different accretionary histories may have played a part in the different trace element chemistries of the resultant CAMP lavas while the isotopic signature of the lavas reflects the incorporation of eroded sediment from adjacent accreted terranes into the mantle by subduction, particularly in northern and transitional CAMP.

The Scranton Rift, as an example of supercontinental inheritance, may have influenced the formation of Pangea by acting as a collisional backstop and leading to a rotation of the direction of subduction. The Scranton Rift may have also influenced the breakup of Pangea as the underplated rift material may have had some structural control over the basins that formed nearby. Additionally geochemical trends showing evidence of more metasomatism of the mantle by subducted sediment melts are observed in the CAMP basalts that were emplaced in the basins north of and adjacent to the Scranton Rift versus the basins located to the South.

Major and trace element chemistry from olivine phenocrysts indicate a pyroxenite component for CAMP basalts based on elevated Ni, low Ca and some elevated Fe/Mn values. Calculated CAMP primary magmas suggest that the source of CAMP may be the result of a reaction between a silica-rich melt and peridotite. Due to the ubiquitous arc signature in CAMP lavas we interpret this pyroxenite component as the result of metasomatism of the upper mantle by previous instances of subduction, possibly in the form of sediment melt.

We suggest that the combination of lithospheric delamination, slab break off, and mantle upwelling is the result of the protracted accretionary history of Pangea, although aspects of this model still require further exploration. For instance, the exact timing of delamination of the Rheic slab is complicated by the extensive erosion in the South and a general lack of consensus on the subduction direction during the final closure of Pangea.

Finally, CAMP is not responsible for the breakup of Pangea, but is itself the result of supercontinental inheritance. As supercontinents are the products of many different processes, it stands to reason that the breakup of each supercontinent will be as unique and complex as the events leading to their formation.

Acknowledgements

This project was supported by NSF GeoPrisms award EAR-1249412 to E. Gazel. The manuscript was improved by the reviews of V. Le Roux, and L. Farmer and benefited from discussions with M. Caddick, W. Whalen and C. Herzberg. Finally we appreciate the editorial comments and handling by C-T. A. Lee.

References

Anderson, D. L. (1982), Hotspots, polar wander, Mesozoic convection and the geoid, *Nature*, *297*(5865), 391-393.

Ackerman, L., N. Mahlen, E. JelÍnek, G. Medaris, J. Ulrych, L. Strnad, and M. MihaljeviČ (2007), Geochemistry and evolution of subcontinental lithospheric mantle in Central Europe: evidence from peridotite xenoliths of the Kozákov volcano, Czech Republic, *Journal of Petrology*, *48*(12), 2235-2260.

Ackerman, L., P. ŠpaČek, T. Magna, J. Ulrych, M. Svojtka, E. Hegner, and K. Balogh (2013), Alkaline and carbonate-rich melt metasomatism and melting of subcontinental lithospheric mantle: evidence from mantle xenoliths, NE Bavaria, Bohemian Massif, *Journal of Petrology*, egt059.

Beattie, P., C. Ford, and D. Russell (1991), Partition coefficients for olivine-melt and orthopyroxene-melt systems, *Contributions to Mineralogy and Petrology*, *109*(2), 212-224.

Bénard, A., and D. A. Ionov (2013), Melt–and fluid–rock interaction in supra-subduction lithospheric mantle: Evidence from andesite-hosted veined peridotite xenoliths, *Journal of Petrology*, egt050.

Benoit, M. H., C. Ebinger, and M. Crampton (2014), Orogenic bending around a rigid Proterozoic magmatic rift beneath the Central Appalachian Mountains, *Earth and Planetary Science Letters*.

Bird, P. (1979), Continental delamination and the Colorado Plateau, *Journal of Geophysical Research: Solid Earth (1978–2012)*, *84*(B13), 7561-7571.

Bertrand, H. (1991), The Mesozoic tholeiitic province of northwest Africa: a volcano-tectonic record of the early opening of Central Atlantic, in *Magmatism in extensional structural settings*, edited, pp. 147-188, Springer.

Bizimis, M., V. J. Salters, M. O. Garcia, and M. D. Norman (2013), The composition and distribution of the rejuvenated component across the Hawaiian plume: Hf-Nd-Sr-Pb isotope systematics of Kaula lavas and pyroxenite xenoliths, *Geochemistry, Geophysics, Geosystems*, *14*(10), 4458-4478.

Blackburn, T. J., P. E. Olsen, S. A. Bowring, N. M. McLean, D. V. Kent, J. Puffer, G. McHone, E. T. Rasbury, and M. Et-Touhami (2013), Zircon U-Pb geochronology links the end-Triassic extinction with the Central Atlantic Magmatic Province, *Science*, *340*(6135), 941-945.

Bullard, E., J. E. Everett, and A. G. Smith (1965), The fit of the continents around the Atlantic, *Philosophical Transactions of the Royal Society of London. Series A, Mathematical and Physical Sciences*, *258*(1088), 41-51.

Callegaro, S., A. Marzoli, H. Bertrand, M. Chiaradia, L. Reisberg, C. Meyzen, G. Bellieni, R. E. Weems, and R. Merle (2013), Upper and lower crust recycling in the source of CAMP basaltic dykes from southeastern North America, *Earth and Planetary Science Letters*, *376*, 186-199.

Callegaro, S., C. Rapaille, A. Marzoli, H. Bertrand, M. Chiaradia, L. Reisberg, G. Bellieni, L. Martins, J. Madeira, and J. Mata (2014), Enriched mantle source for the Central Atlantic magmatic province: new supporting evidence from Southwestern Europe, *Lithos*, *188*, 15-32.

Campbell, I. H. (2007), Testing the plume theory, *Chemical Geology*, *241*(3–4), 153-176.

Carpentier, M., C. Chauvel, and N. Mattielli (2008), Pb–Nd isotopic constraints on sedimentary input into the Lesser Antilles arc system, *Earth and Planetary Science Letters*, *272*(1), 199-211.

Cebriá, J. M., J. López-Ruiz, M. Doblas, L. T. Martins, and J. Munha (2003), Geochemistry of the Early Jurassic Messejana–Plasencia dyke (Portugal–Spain); Implications on the Origin of the Central Atlantic Magmatic Province *Journal of Petrology*, *44*(3), 21.

Chalot-Prat, F., and A.-M. Boullier (1997), Metasomatism in the subcontinental mantle beneath the Eastern Carpathians (Romania): new evidence from trace element geochemistry, *Contributions to Mineralogy and Petrology*, *129*(4), 284-307.

Class, C., D. M. Miller, S. L. Goldstein, and C. H. Langmuir (2000), Distinguishing melt and fluid subduction components in Umnak Volcanics, Aleutian Arc, *Geochemistry, Geophysics, Geosystems*, *1*(6).

Cloos, M., B. Sapiie, A. Q. van Ufford, R. J. Weiland, P. Q. Warren, and T. P. McMahon (2005), Collisional delamination in New Guinea: The geotectonics of subducting slab breakoff, *Geological Society of America Special Papers*, *400*, 1-51.

Coltice, N., B. Phillips, H. Bertrand, Y. Ricard, and P. Rey (2007), Global warming of the mantle at the origin of flood basalts over supercontinents, *Geology*, *35*(5), 391-394.

Coltice, N., H. Bertrand, P. Rey, F. Jourdan, B. R. Phillips, and Y. Ricard (2009), Global warming of the mantle beneath continents back to the Archaean, *Gondwana Research*, *15*(3), 254-266.

Coney, P. J., D. L. Jones, and J. W. Monger (1980), Cordilleran suspect terranes, *Nature*, *288*(5789), 329-333.

Conrad, C. P., and P. Molnar (1997), The growth of Rayleigh—Taylor-type instabilities in the lithosphere for various rheological and density structures, *Geophysical Journal International*, *129*(1), 95-112.

Courtillot, V., C. Jaupart, I. Manighetti, P. Tapponnier, and J. Besse (1999), On causal links between flood basalts and continental breakup, *Earth and Planetary Science Letters*, *166*(3–4), 177-195.

Courtillot, V. E., and P. R. Renne (2003), On the ages of flood basalt events, *Comptes Rendus Geoscience*, *335*(1), 113-140.

Currie, K., J. Whalen, W. Davis, F. Longstaffe, and B. Cousens (1998), Geochemical evolution of peraluminous plutons in southern Nova Scotia, Canada—a pegmatite-poor suite, *Lithos*, *44*(3), 117-140.

Danyushevsky, L. V., and P. Plechov (2011), Petrolog3: Integrated software for modeling crystallization processes, *Geochemistry, Geophysics, Geosystems*, *12*(7).

Davidson, J., S. Turner, and T. Plank (2013), Dy/Dy*: variations arising from mantle sources and petrogenetic processes, *Journal of Petrology*, *54*(3), 525-537.

Davy, B. (2014), Rotation and offset of the Gondwana convergent margin in the New Zealand region following Cretaceous jamming of Hikurangi Plateau large igneous province subduction, *Tectonics*, *33*(8), 1577-1595.

De Min, A., E. M. Piccirillo, A. Marzoli, G. Bellieni, P. R. Renne, M. Ernesto, and L. S. Marques (2003), The Central Atlantic Magmatic Province (CAMP) in Brazil: petrology, geochemistry, 40Ar/39Ar ages, paleomagnetism and geodynamic implications, *The central Atlantic magmatic province: insights from fragments of Pangea*, 91-128.

Deckart, K., H. Bertrand, and J.-P. Liégeois (2005), Geochemistry and Sr, Nd, Pb isotopic composition of the Central Atlantic Magmatic Province (CAMP) in Guyana and Guinea, *Lithos*, *82*(3), 289-314.

Dorais, M. J., M. Harper, S. Larson, H. Nugroho, P. Richardson, and N. Roosmawati (2005), A comparison of Eastern North America and Coastal New England magma suites: implications for subcontinental mantle evolution and the broad-terrane hypothesis, *Canadian Journal of Earth Sciences*, *42*(9), 1571-1587.

Dorais, M. J., and M. Tubrett (2008), Identification of a subduction zone component in the Higganum dike, Central Atlantic Magmatic Province: A LA-ICPMS study of clinopyroxene with implications for flood basalt petrogenesis, *Geochemistry, Geophysics, Geosystems*, *9*(10).

Dostal, J., and M. Durning (1998), Geochemical constraints on the origin and evolution of early Mesozoic dikes in Atlantic Canada, *European Journal of Mineralogy*, *10*(1), 79-93.

Ernst, R. E., and K. L. Buchan (2002), Maximum size and distribution in time and space of mantle plumes: evidence from large igneous provinces, *Journal of Geodynamics*, *34*(2), 309-342.

Elkins-Tanton, L. T. (2005), Continental magmatism caused by lithospheric delamination, *Geological Society of America Special Papers*, *388*, 12.

Faill, R. T. (2003), The early Mesozoic Birdsboro central Atlantic margin basin in the Mid-Atlantic region, eastern United States, *Geological Society of America Bulletin*, *115*(4), 406-421.

Foley, S. F., D. Prelevic, T. Rehfeldt, and D. E. Jacob (2013), Minor and trace elements in olivines as probes into early igneous and mantle melting processes, *Earth and Planetary Science Letters*, *363*, 181-191.

Fokin, M. A. (2003), Space-time analysis of magmatism: the igneous record for an early Cryogenian plume track in central Appalachian orogen, Virginia Polytechnic Institute and State University.

Frizon de Lamotte, D., B. Fourdan, S. Leleu, F. Leparmentier, and P. Clarens (2015), Style of rifting and the stages of Pangea breakup, *Tectonics*.

Gale, A., C. A. Dalton, C. H. Langmuir, Y. Su, and J. G. Schilling (2013), The mean composition of ocean ridge basalts, *Geochemistry, Geophysics, Geosystems*, *14*(3), 489-518.

Gazel, E., K. Hoernle, M. J. Carr, C. Herzberg, I. Saginor, P. v. den Bogaard, F. Hauff, M. Feigenson, and C. Swisher III (2011), Plume–subduction interaction in southern Central America: Mantle upwelling and slab melting, *Lithos*, *121*(1), 117-134.

Gazel, E., Hayes, J., Hoernle, K., Everson, E., Holbrooke, W. S., Kelemen, P., Hauff, F., van den Bogaard, P., Vance, E., Chu, S., Yogodzinski, G. Generation of continental crust in oceanic arcs, **Nature** Geoscience 8, 321-327**.**

Greenough, J. D., A. Hayatsu, and V. S. Papezik (1988), Mineralogy, petrology and geochemistry of the alkaline Malpeque Bay sill, Prince Edward Island, *Canadian Mineralogist*, *26*, 97-108.

Hall, J., F. Marillier, and S. Dehler (1998), Geophysical studies of the structure of the Appalachian orogen in the Atlantic borderlands of Canada, *Canadian Journal of Earth Sciences*, *35*(11), 1205-1221.

Hatcher, R. D. (2002), Alleghanian (Appalachian) orogeny, a product of zipper tectonics: Rotational transpressive continent-continent collision and closing of ancient oceans along irregular margins, *Special paper-Geological Society of America*(364), 199-208.

Hatcher, R. D. (2010), The Appalachian orogen: A brief summary, *Geological Society of America Memoirs*, *206*, 1-19.

Hawkesworth, C., K. Gallagher, J. Hergt, and F. McDermott (1993), Mantle and slab contribution in arc magmas, *Annual Review of Earth and Planetary Sciences*, *21*, 175-204.

Hawkesworth, C., S. Turner, F. McDermott, D. Peate, and P. Van Calsteren (1997), U-Th isotopes in arc magmas: Implications for element transfer from the subducted crust, *Science*, *276*(5312), 551-555.

Hawman, R. B. (2008), Crustal thickness variations across the Blue Ridge Mountains, southern Appalachians: An alternative procedure for migrating wide-angle reflection data, *Bulletin of the Seismological Society of America*, *98*(1), 469-475.

Herzberg, C. (2010), Identification of Source Lithology in the Hawaiian and Canary Islands: Implications for Origins, *Journal of Petrology*.

Herzberg, C. (2011), Identification of source lithology in the Hawaiian and Canary Islands: Implications for origins, *Journal of Petrology*, *52*(1), 113-146.

Herzberg, C., and M. O'hara (2002), Plume-associated ultramafic magmas of Phanerozoic age, *Journal of Petrology*, *43*(10), 1857-1883.

Herzberg, C., and P. D. Asimow (2008), Petrology of some oceanic island basalts: PRIMELT2.XLS software for primary magma calculation, *Geochemistry, Geophysics, Geosystems*, *9*(9), n/a-n/a.

Herzberg, C., and E. Gazel (2009), Petrological evidence for secular cooling in mantle plumes, *Nature*, *458*(7238), 619-622.

Herzberg, C., W. Fyfe, and M. Carr (1983), Density constraints on the formation of the continental Moho and crust, *Contributions to Mineralogy and Petrology*, *84*(1), 1-5.

Herzberg, C., R. Cabral, M. Jackson, C. Vidito, J. Day, and E. Hauri (2014), Phantom Archean crust in Mangaia hotspot lavas and the meaning of heterogeneous mantle, *Earth and Planetary Science Letters*, *396*, 97-106.

Herzberg, C., P. D. Asimow, D. A. Ionov, C. Vidito, M. G. Jackson, and D. Geist (2013), Nickel and helium evidence for melt above the core-mantle boundary, *Nature*, *493*(7432), 393-397.

Hibbard, J. P., C. R. Van Staal, and D. W. Rankin (2007), A comparative analysis of pre-Silurian crustal building blocks of the northern and the southern Appalachian orogen, *American Journal of Science*, *307*(1), 23-45.

Hibbard, J. P., C. R. van Staal, and D. W. Rankin (2010), Comparative analysis of the geological evolution of the northern and southern Appalachian orogen: Late Ordovician-Permian, *Geological Society of America Memoirs*, *206*, 51-69.

Hill, R. I. (1991), Starting plumes and continental break-up, *Earth and Planetary Science Letters*, *104*(2), 398-416.

Hirschmann, M., P. D. Asimow, M. Ghiorso, and E. Stolper (1999), Calculation of peridotite partial melting from thermodynamic models of minerals and melts. III. Controls on isobaric melt production and the effect of water on melt production, *Journal of Petrology*, *40*(5), 831-851.

Hodych, J., and A. Hayatsu (1980), K-Ar isochron age and paleomagnetism of diabase along the trans-Avalon aeromagnetic lineament-evidence of Late Triassic rifting in Newfoundland, *Canadian Journal of Earth Sciences*, *17*(4), 491-499.

Hofmann, A., K. Jochum, M. Seufert, and W. White (1986), Nb and Pb in oceanic basalts: new constraints on mantle evolution, *Earth and Planetary Science Letters*, *79*(1), 33-45.

Hofmann, A. W. (2007), 2.03 - Sampling Mantle Heterogeneity through Oceanic Basalts: Isotopes and Trace Elements, in *Treatise on Geochemistry*, edited by H. D. Holland and K. K. Turekian, pp. 1-44, Pergamon, Oxford.

Hole, M. J. (2015), The generation of continental flood basalts by decompression melting of internally heated mantle, *Geology*, G36442. 36441.

Holm, P. M., J. R. Wilson, B. P. Christensen, L. Hansen, S. L. Hansen, K. M. Hein, A. K. Mortensen, R. Pedersen, S. Plesner, and M. K. Runge (2005), Sampling the Cape Verde mantle plume: evolution of melt compositions on Santo Antão, Cape Verde Islands, *Journal of Petrology*.

Houseman, G. A., and P. Molnar (1997), Gravitational (Rayleigh–Taylor) instability of a layer with non-linear viscosity and convective thinning of continental lithosphere, *Geophysical Journal International*, *128*(1), 125-150.

Houseman, G. A., D. McKenzie, and P. Molnar (1981), Convective instability of a thickened boundary layer and its relevance for the thermal evolution of continental convergent belts, *Journal of Geophysical Research: Solid Earth (1978–2012)*, *86*(B7), 6115-6132.

Janney, P. E., and P. R. Castillo (2001), Geochemistry of the oldest Atlantic oceanic crust suggests mantle plume involvement in the early history of the central Atlantic Ocean, *Earth and Planetary Science Letters*, *192*(3), 291-302.

Jourdan, F., A. Marzoli, H. Bertrand, M. Cosca, and D. Fontignie (2003), The Northernmost CAMP: 40Ar/39Ar Age, Petrology and Sr-Nd-Pb Isotope Geochemistry of the Kerforne Dike, Brittany, France, *The Central Atlantic Magmatic Province: Insights from Fragments of Pangea*, 209-226.

Jull, M., and P. Kelemen (2001), On the conditions for lower crustal convective instability, *Journal of Geophysical Research: Solid Earth (1978–2012)*, *106*(B4), 6423-6446.

Kay, R. W., and S. Kay (1993), Delamination and delamination magmatism, *Tectonophysics*, *219*(1), 177-189.

Kelemen, P. B., G. M. Yogodzinski, and D. W. Scholl (2003), Along-strike variation in the Aleutian island arc: Genesis of high Mg# andesite and implications for continental crust, *Inside the Subduction Factory, Geophys. Monogr. Ser*, *138*, 223-276.

Keppie, D. F., C. A. Currie, and C. Warren (2009), Subduction erosion modes: comparing finite element numerical models with the geological record, *Earth and Planetary Science Letters*, *287*(1), 241-254.

King, S. D., and D. L. Anderson (1995), An alternative mechanism of flood basalt formation, *Earth and Planetary Science Letters*, *136*(3–4), 269-279.

Kogiso, T., M. Hirschmann, and M. Pertermann (2004), High-pressure partial melting of mafic lithologies in the mantle, *Journal of Petrology*, *45*(12), 2407-2422.

Lefort, J.-P., and R. Van der Voo (1981), A kinematic model for the collision and complete suturing between Gondwanaland and Laurussia in the Carboniferous, *The Journal of Geology*, 537-550.

Lenoir, X., C. J. Garrido, J.-L. Bodinier, and J.-M. Dautria (2000), Contrasting lithospheric mantle domains beneath the Massif Central (France) revealed by geochemistry of peridotite xenoliths, *Earth and Planetary Science Letters*, *181*(3), 359-375.

Levin, V., J. Park, M. T. Brandon, and W. Menke (2000), Thinning of the upper mantle during late Paleozoic Appalachian orogenesis, *Geology*, *28*(3), 239-242.

Li, C., and E. M. Ripley (2010), The relative effects of composition and temperature on olivine-liquid Ni partitioning: Statistical deconvolution and implications for petrologic modeling, *Chemical Geology*, *275*(1), 99-104.

Lustrino, M. (2005), How the delamination and detachment of lower crust can influence basaltic magmatism, *Earth-Science Reviews*, *72*(1–2), 21-38.

Mahmoudi, A., and H. Bertrand (2007), Geochemical identification of the central Atlantic magmatic province in folded domain, exemplified by the Moroccan Middle Atlas, *Comptes Rendus Géosciences*, *339*, 545-552.

Martins, L., J. Madeira, N. Youbi, J. Munhá, J. Mata, and R. Kerrich (2008), Rift-related magmatism of the Central Atlantic magmatic province in Algarve, Southern Portugal, *Lithos*, *101*(1), 102-124.

Marzoli, A., P. R. Renne, E. M. Piccirillo, M. Ernesto, G. Bellieni, and A. D. Min (1999), Extensive 200-Million-Year-Old Continental Flood Basalts of the Central Atlantic Magmatic Province, *Science*, *284*(5414), 616-618.

Marzoli, A., H. Bertrand, K. B. Knight, S. Cirilli, N. Buratti, C. Vérati, S. Nomade, P. R. Renne, N. Youbi, and R. Martini (2004), Synchrony of the Central Atlantic magmatic province and the Triassic-Jurassic boundary climatic and biotic crisis, *Geology*, *32*(11), 973-976.

Marzoli, A., F. Jourdan, J. H. Puffer, T. Cuppone, L. H. Tanner, R. E. Weems, H. Bertrand, S. Cirilli, G. Bellieni, and A. De Min (2011), Timing and duration of the Central Atlantic magmatic province in the Newark and Culpeper basins, eastern USA, *Lithos*, *122*(3), 175-188.

Matzen, A. K., M. B. Baker, J. R. Beckett, and E. M. Stolper (2013), The temperature and pressure dependence of nickel partitioning between olivine and silicate melt, *Journal of Petrology*, *54*(12), 2521-2545.

May, P. R. (1971), Pattern of Triassic-Jurassic diabase dikes around the North Atlantic in the context of predrift position of the continents, *Geological Society of America Bulletin*, *82*(5), 1285-1292.

Mazza, S. E., E. Gazel, E. A. Johnson, M. J. Kunk, R. McAleer, J. A. Spotila, M. Bizimis, and D. S. Coleman (2014), Volcanoes of the passive margin: The youngest magmatic event in eastern North America, *Geology*, *42*(6), 483-486.

McClellan, E., and E. Gazel (2014), The Cryogenian intra-continental rifting of Rodinia: Evidence from the Laurentian margin in eastern North America, *Lithos*, *206–207*(0), 321-337.

McDonough, W. F., and S.-S. Sun (1995), The composition of the Earth, *Chemical geology*, *120*(3), 223-253.

McHone, J. G. (1992), Mafic dike suites within Mesozoic igneous provinces of New England and Atlantic Canada, *Geological Society of America Special Papers*, *268*, 1-12.

McHone, J. G. (2000), Non-plume magmatism and rifting during the opening of the central Atlantic Ocean, *Tectonophysics*, *316*(3-4), 9.

McHone, J. G. (2003), Volatile emissions from Central Atlantic Magmatic Province Basalts: Mass assumptions and environmental consequences, *136*, 241-254.

McHone, J. G., and J. R. Butler (1984), Mesozoic igneous provinces of New England and the opening of the North Atlantic Ocean, *Geological Society of America Bulletin*, *95*(7), 757-765.

Merle, R., A. Marzoli, H. Bertrand, L. Reisberg, C. Verati, C. Zimmermann, M. Chiaradia, G. Bellieni, and M. Ernesto (2011), $^{40}Ar/^{39}Ar$ ages and Sr–Nd–Pb–Os geochemistry of CAMP tholeiites from Western Maranhão basin (NE Brazil), *Lithos*, *122*(3), 137-151.

Merle, R., A. Marzoli, L. Reisberg, H. Bertrand, A. Nemchin, M. Chiaradia, S. Callegaro, F. Jourdan, G. Bellieni, and D. Kontak (2013), Sr, Nd, Pb and Os isotope systematics of CAMP tholeiites from Eastern North America (ENA): Evidence of a subduction-enriched mantle source, *Journal of Petrology*, egt063.

Missenard, Y., and A. Cadoux (2012), Can Moroccan Atlas lithospheric thinning and volcanism be induced by Edge-Driven Convection?, *Terra Nova*, *24*(1), 27-33.

Morgan, W. J. (1983), Hotspot tracks and the early rifting of the Atlantic, *Tectonophysics*, *94*(1), 123-139.

Moran, P. C., S. M. Barr, C. E. White, and M. A. Hamilton (2007), Petrology, age, and tectonic setting of the Seal Island Pluton, offshore southwestern Nova Scotia, *Canadian Journal of Earth Sciences*, *44*(10), 1467-1478.

Morency, C., M.-P. Doin, and C. Dumoulin (2002), Convective destabilization of a thickened continental lithosphere, *Earth and Planetary Science Letters*, *202*(2), 303-320.

Murphy, J. B., J. Dostal, G. Gutiérrez-Alonso, and J. D. Keppie (2011), Early Jurassic magmatism on the northern margin of CAMP: Derivation from a Proterozoic sub-continental lithospheric mantle, *Lithos*, *123*(1), 158-164.

Navon, O., and E. Stolper (1987), Geochemical consequences of melt percolation: the upper mantle as a chromatographic column, *The Journal of Geology*, 285-307.

Nelson, K. (1992), Are crustal thickness variations in old mountain belts like the Appalachians a consequence of lithospheric delamination?, *Geology*, *20*(6), 498-502.

Niu, Y., M. Wilson, E. R. Humphreys, and M. J. O'Hara (2011), The origin of intra-plate ocean island basalts (OIB): the lid effect and its geodynamic implications, *Journal of Petrology*, *52*(7-8), 1443-1468.

O'hara, M. (1968), The bearing of phase equilibria studies in synthetic and natural systems on the origin and evolution of basic and ultrabasic rocks, *Earth-Science Reviews*, *4*, 69-133.

Olsen, P. E. (1997), Stratigraphic record of the early Mesozoic breakup of Pangea in the Laurasia-Gondwana rift system, *Annual Review of Earth and Planetary Sciences*, *25*(1), 337-401.

Olsen, P. E., R. Schlische, and P. Gore (1989), Tectonic, depositional, and paleoecological history of early Mesozoic rift basins, eastern North America, *Int. Geol. Cong. Field Trip Guidebook*, *351*, 1989.

Ong, P. F., B. A. Van der Pluijm, and R. Van der Voo (2007), Early rotation and late folding in the Pennsylvania salient (US Appalachians): Evidence from calcite-twinning analysis of Paleozoic carbonates, *Geological Society of America Bulletin*, *119*(7-8), 796-804.

Pegram, W. J. (1990), Development of continental lithospheric mantle as reflected in the chemistry of the Mesozoic Appalachian tholeiites, USA, *Earth and Planetary Science Letters*, *97*(3), 316-331.

Pe-Piper, G., and L. F. Jansa (1986), Triassic olivine-normative diabase from Northumberland Strait, eastern Canada: implications for continental rifting, *Canadian Journal of Earth Sciences*, *23*(7), 1013-1021.

Pe-Piper, G., and D. J. Piper (1998), Geochemical evolution of Devonian-Carboniferous igneous rocks of the Magdalen basin, eastern Canada: Pb-and Nd-isotope evidence for mantle and lower crustal sources, *Canadian Journal of Earth Sciences*, *35*(3), 201-221.

Pe-Piper, G., and P. H. Reynolds (2000), Early Mesozoic alkaline mafic dykes, southwestern Nova Scotia, Canada, and their bearing on Triassic–Jurassic magmatism, *The Canadian Mineralogist*, *38*(1), 217-232.

Pe-Piper, G., L. F. Jansa, and R. S. J. Lambert (1992), Early Mesozoic magmatism on the eastern Canadian margin: Petrogenetic and tectonic significance, *Geological Society of America Special Papers*, *268*, 13-36.

Pearce, J., and D. Peate (1995), Tectonic implications of the composition of volcanic arc magmas, *Annual Review of Earth and Planetary Sciences*, *23*, 251-286.

Pearce, J. A. (2008), Geochemical fingerprinting of oceanic basalts with applications to ophiolite classification and the search for Archean oceanic crust, *Lithos*, *100*(1), 14-48.

Pettingill, H. S., A. Sinha, and M. Tatsumoto (1984), Age and origin of anorthosites, charnockites, and granulites in the central Virginia Blue Ridge: Nd and Sr isotopic evidence, *Contributions to Mineralogy and Petrology*, *85*(3), 279-291.

Plank, T. (2005), Constraints from thorium/lanthanum on sediment recycling at subduction zones and the evolution of the continents, *Journal of Petrology*, *46*(5), 921-944.

Plank, T. (2005), Constraints from thorium/lanthanum on sediment recycling at subduction zones and the evolution of the continents, *Journal of Petrology*, *46*(5), 921-944.

Plank, T., K. A. Kelley, M. M. Zimmer, E. H. Hauri, and P. J. Wallace (2013), Why do mafic arc magmas contain~ 4wt% water on average?, *Earth and Planetary Science Letters*, *364*, 168-179.

Plank, T. (2014), 4.17 - The Chemical Composition of Subducting Sediments, in *Treatise on Geochemistry (Second Edition)*, edited by H. D. H. K. Turekian, pp. 607-629, Elsevier, Oxford.

Puffer, J. H. (2001), Contrasting high field strength element contents of continental flood basalts from plume versus reactivated-arc sources, *Geology*, *29*(8), 675-678.

Puffer, J. H. (2003), A Reactivated Backield strength element cgma, *The Central Atlantic Magmatic Province: Insights from Fragments of Pangea*, 151-162.

Qin, L., and M. Humayun (2008), The Fe/Mn ratio in MORB and OIB determined by ICP-MS, *Geochimica et Cosmochimica Acta*, *72*(6), 1660-1677.

Reynolds, P., P. Elias, G. Muecke, and A. Grist (1987), Thermal history of the southwestern Meguma zone, Nova Scotia, from an 40Ar/39Ar and fission track dating study of intrusive rocks, *Canadian Journal of Earth Sciences*, *24*(10), 1952-1965.

Roeder, P., and R. Emslie (1970), Olivine-liquid equilibrium, *Contributions to mineralogy and petrology*, *29*(4), 275-289.

Ross, M. E. (1992), Petrology and tectonic significance of Mesozoic mafic dikes of the coastal New England igneous province, Massachusetts, *Geological Society of America Special Papers*, *268*, 63-74.

Ross, M. E. (2010), An Early Triassic 40Ar/39Ar age for a camptonite dyke in Cambridge, Massachusetts, *Atlantic Geology*, *46*, 127-135.

Ruiz-Martínez, V. C., T. H. Torsvik, D. J. van Hinsbergen, and C. Gaina (2012), Earth at 200Ma: Global palaeogeography refined from CAMP palaeomagnetic data, *Earth and Planetary Science Letters*, *331*, 67-79.

Sacks, P. E., and D. T. Secor (1990), Delamination in collisional orogens, *Geology*, *18*(10), 999-1002.

Samson, S. D., D. G. Coler, and J. A. Speer (1995), Geochemical and NdSrPb isotopic composition of Alleghanian granites of the southern Appalachians: Origin, tectonic setting, and source characterization, *Earth and Planetary Science Letters*, *134*(3), 359-376.

Schlische, R. W., and P. E. Olsen (1990), Quantitative filling model for continental extensional basins with applications to early Mesozoic rifts of eastern North America, *The Journal of Geology*, 135-155.

Schlische, R. W., M. O. Withjack, and P. E. Olsen (2003), Relative timing of CAMP, rifting, continental breakup, and basin inversion: tectonic significance, *The Central Atlantic Magmatic Province: Insights from Fragments of Pangea*, 33-59.

Schott, B., and H. Schmeling (1998), Delamination and detachment of a lithospheric root, *Tectonophysics*, *296*(3), 225-247.

Schott, B., D. A. Yuen, and H. Schmeling (2000), The significance of shear heating in continental delamination, *Physics of the Earth and Planetary Interiors*, *118*(3), 273-290.

Sinha, A., J. Hogan, and J. Parks (1996), Lead isotope mapping of crustal reservoirs within the Grenville Superterrane: I. Central and Southern Appalachians, *Earth Processes: Reading the Isotopic Code*, 293-305.

Sobolev, A. V., A. W. Hofmann, S. V. Sobolev, and I. K. Nikogosian (2005), An olivine-free mantle source of Hawaiian shield basalts, *Nature*, *434*(7033), 590-597.

Sobolev, A. V., et al. (2007), The Amount of Recycled Crust in Sources of Mantle-Derived Melts, *Science*, *316*(5823), 412-417.

Steiger, R. H., and E. Jäger (1977), Subcommission on geochronology: convention on the use of decay constants in geo-and cosmochronology, *Earth and planetary science letters*, *36*(3), 359-362.

Stern, C. R. (2011), Subduction erosion: rates, mechanisms, and its role in arc magmatism and the evolution of the continental crust and mantle, *Gondwana Research*, *20*(2), 284-308.

Storey, B. C. (1995), The role of mantle plumes in continental breakup: case histories from Gondwanaland, *Nature*, *377*(6547), 301-308.

Sun, S.-S., and W. McDonough (1989), Chemical and isotopic systematics of oceanic basalts: implications for mantle composition and processes, *Geological Society, London, Special Publications*, *42*(1), 313-345.

Sundeen, D. A., and M. C. Huff (1992), Petrography, petrology, and K-Ar geochronology of hypabyssal mafic and silicic Mesozoic igneous rocks in southeastern New Hampshire, *Geological Society of America Special Papers*, *268*, 75-94

Swanson, M. T. (1992), Structural sequence and tectonic significance of Mesozoic dikes in southern coastal Maine, *Geological Society of America Special Papers*, *268*, 37-62.

Tanton, L. T. E., and B. H. Hager (2000), Melt intrusion as a trigger for lithospheric foundering and the eruption of the Siberian flood basalts, *Geophysical research letters*, *27*(23), 3937-3940.

Tarduno, J., H. Mayer, E. Winterer, W. Sliter, L. Kroenke, J. Mahoney, M. Leckie, R. Musgrave, and M. Storey (1991), Rapid formation of Ontong Java Plateau by Aptian mantle plume volcanism, *Science*, *254*(5030), 399-403.

Toplis, M. (2005), The thermodynamics of iron and magnesium partitioning between olivine and liquid: criteria for assessing and predicting equilibrium in natural and experimental systems, *Contributions to Mineralogy and Petrology*, *149*(1), 22-39.

van Staal, C. R., J. B. Whalen, P. Valverde-Vaquero, A. Zagorevski, and N. Rogers (2009), Pre-Carboniferous, episodic accretion-related, orogenesis along the Laurentian margin of the northern Appalachians, *Geological Society, London, Special Publications*, *327*(1), 271-316.

Verati, C., H. Bertrand, and G. Féraud (2005), The farthest record of the Central Atlantic Magmatic Province into West Africa craton: Precise 40 Ar/39 Ar dating and geochemistry of Taoudenni basin intrusives (northern Mali), *Earth and Planetary Science Letters*, *235*(1), 391-407.

Wagner, L. S., K. Stewart, and K. Metcalf (2012), Crustal-scale shortening structures beneath the Blue Ridge Mountains, North Carolina, USA, *Lithosphere*, *4*(3), 242-256.

Wang, Z., and G. A. Gaetani (2008), Partitioning of Ni between olivine and siliceous eclogite partial melt: experimental constraints on the mantle source of Hawaiian basalts, *Contributions to Mineralogy and Petrology*, *156*(5), 661-678.

Weigand, P. W., and P. C. Ragland (1970), Geochemistry of Mesozoic dolerite dikes from eastern North America, *Contributions to Mineralogy and Petrology*, *29*(3), 195-214.

White, R., and D. McKenzie (1989), Magmatism at Rift Zones: The Generation of Volcanic Continental Margins and Flood Basalts, *Journal of Geophysical Research*, *94*(B6), 44.

White, W. M., and B. Dupré (1986), Sediment subduction and magma genesis in the Lesser Antilles: isotopic and trace element constraints, *Journal of Geophysical Research: Solid Earth (1978–2012)*, *91*(B6), 5927-5941.

Wilson, J. T. (1965), A New Class of Faults and their Bearing on Continental Drift, *Nature*, *207*(4995), 343-347.

Wilson, J. T. (1966), Did the Atlantic Close and then Re-Open?, *Nature*, *211*(5050), 676-681.

Wilson, M. (1997), Thermal evolution of the Central Atlantic passive margins: continental break-up above a Mesozoic super-plume, *Journal of the Geological Society*, *154*(3), 491-495.

Wise, D. U. (2004), Pennsylvania salient of the Appalachians: A two-azimuth transport model based on new compilations of Piedmont data, *Geology*, *32*(9), 777-780.

Withjack, M. O., P. E. Olsen, and R. W. Schlische (1995), Tectonic evolution of the Fundy rift basin, Canada: evidence of extension and shortening during passive margin development, *Tectonics*, *14*(2), 390-405.

Woodcock, N., N. Soper, and R. Strachan (2007), A Rheic cause for the Acadian deformation in Europe, *Journal of the Geological Society*, *164*(5), 1023-1036.

Woodhead, J., J. Hergt, J. Davidson, and S. Eggins (2001), Hafnium isotope evidence for 'conservative'element mobility during subduction zone processes, *Earth and Planetary Science Letters*, *192*(3), 331-346.

Wortel, M., and W. Spakman (2000), Subduction and slab detachment in the Mediterranean-Carpathian region, *Science*, *290*(5498), 1910-1917.

Zhang, H.-F., Y.-L. Sun, Y.-J. Tang, Y. Xiao, W.-H. Zhang, X.-M. Zhao, M. Santosh, and M. A. Menzies (2012), Melt-peridotite interaction in the Pre-Cambrian mantle beneath the western North China Craton: Petrology, geochemistry and Sr, Nd and Re isotopes, *Lithos*, *149*, 100-114.

Figure Captions

Figure 1. Map of CAMP modified from *Deckart et al.* [2005]. Continents are in the pre-rift configuration of Pangea after *Bullard et al.* [1965]. CAMP exposures and boundary after *McHone* [2003]. Mesozoic rift basin locations: F, Fundy; A, Argana;

DF, Deerfield; H, Hartford; P, Pomperaug; N, Newark; G, Gettysburg; C, Culpepper; T, Taylorsville; NO, Norfolk; R, Richmond; FM, Farmville; D, Danville; DR, Deep River from *Schlische et al.* [2003] and *Olsen* [1997]. Accreted terrane boundaries from *Hibbard et al.* [2010] and *Hatcher* [2010]. It should be noted that the extension of the Carolina terrane to the North and East beneath the coastal plain is based on subsurface data and is much less certain [*Hatcher*, 2010]. Alternatively the more northern portion of Carolina could be part of Avalonia [*Hatcher*, 2010]. The Scranton Rift location from *Benoit et al.* [2014].

Figure 2. Rifting and sediment depositional history of Mesozoic rift basins after *Olsen* [1997]. Rift basins from left to right: northern basins: F, Fundy; A, Argana; DF, Deerfield; H, Hartford; P, Pomperaug; transitional basins: N, Newark; G, Gettysburg; C, Culpepper; southern basins: T, Taylorsville; R, Richmond; N, Norfolk; FM, Farmville; D, Danville/Deep River; DR, Deep River; SG, South Georgia. The average age of CAMP and timing of the End Triassic Extinction (ETE) are from *Blackburn et al.* [2013]. Rifting and deposition begins and ends earlier in the southern than in the northern basins. Deposition in the Newark, Gettysburg, and Culpepper basins begins in the Late Triassic, as in the case with the southern basins, but continues into the Jurassic like the northern basins. Additionally synrift CAMP flows are absent from the southern rift basins. Age constraints for basin fill rely on biostratigraphy, paleomagnetic data and Milankovitch cyclicity and are poorly constrained [Olsen,

1997]. Shown here are the best estimates of maximum ages based on the available information.

Figure 3. Multi element diagram normalized to primitive mantle after *McDonough and Sun* [1995] comparing CAMP to a Marianas arc average from *Gazel et al.* [2015] and representative samples from the Ontong Java oceanic plateau (data from the GEOROC database http://georoc.mpch-mainz.gwdg.de/georoc/). CAMP samples have both Nb and Ta depletions as well as LILE enrichments similar to the Marianas arc average, but differing from Ontong Java plateau, which is plume-derived [e.g., *Tarduno et al.*, 1991].

Figure 4. Age corrected (200 Ma) Sr-Nd-Pb radiogenic isotopes for samples from Africa [*Bertrand*, 1991; *Marzoli et al.*, 2004; *Deckart et al.*, 2005; *Verati et al.*, 2005; *Mahmoudi and Bertrand*, 2007] and Europe [*Cebriá et al.*, 2003; *Jourdan et al.*, 2003; *Martins et al.*, 2008; *Callegaro et al.*, 2014] plot alongside northern and transitional CAMP [*Dostal and Durning*, 1998; *Marzoli et al.*, 2011; *Merle et al.*, 2013]. South American CAMP [*Deckart et al.*, 2005; *Merle et al.*, 2011] lavas plot with northern and transitional CAMP or depleted MORB mantle (DMM) and Global Average MORB [*Gale et al.*, 2013] indicative of the transition to oceanic crust [*Deckart et al.*, 2005].

Coastal New England Province lavas are from *Pe-Piper and Reynolds* [2000] and *Dorais et al.* [2005]. Global average MORB from *Gale et al.* [2013]. Location of mantle reservoirs HIMU (high μ = $^{238}U/^{204}Pb$), depleted MORB mantle (DMM), enriched mantle I (EMI) and enriched mantle II (EMII) after *Hofmann* [2007]. Additional southern CAMP data from *Callegaro et al.* [2013] and *Mazza et al.* [2014]. Additional CAMP data can be found in Table S4. Radiogenic isotope ratios were age corrected to initial eruptive values at 200 Ma assuming parent/daughter values reported in Tables S1 and S4 and decay constants from *Steiger and Jäger* [1977].

Figure 5. Trace element data from CAMP olivine phenocrysts plotted versus Mg# ([molar MgO/FeO+MgO]*100%). A) CAMP samples plot alongside data from Mauna Kea and above samples from Indian and Pacific MORB [*Sobolev et al.*, 2007] suggesting a pyroxenite component. B) CAMP data plots within the peridotite-derived field, but also at elevated Fe/Mn values indicating a pyroxenite component. C) CAMP data plots at lower Ca values than expected for peridotite-derived melts further supporting a pyroxenite component in the source. Diagrams modified from *Herzberg* [2011].

Figure 6. Trace element comparison of northern, southern and transitional CAMP. The Lesser Antilles and Marianas arcs were selected for comparison as the terranes accreted to the Laurentian margin were most likely island arcs [*Hatcher*, 2010]. The Cascades arc was included because it developed on previously accreted terranes [e.g. *Coney et al.*, 1980] making it similar to the arcs that may have developed on the Laurentian margin. A) Th/Yb-Nb/Yb diagram after *Pearce* [2008] showing CAMP lavas plotting above the mantle array along with arc samples . B) Ce/Yb-Nb/U plot for northern, transitional and southern CAMP. The small group of northern and transitional CAMP samples with lower Ce/Yb, Th/Yb, and Nb/U ratios are younger pulses of CAMP [*Blackburn et al.*, 2013]. Additional CAMP data in Table S4 from *Bertrand*, 1991; *Dostal and Durning*, 1998; *Puffer and Volkert*, 2001; *Cebriá et al.*, 2003; *Jourdan et al.*, 2003; *Marzoli et al.*, 2004; *Deckart et al.*, 2005; *Verati et al.*, 2005; *Mahmoudi and Bertrand*, 2007; *Martins et al.*, 2008; *Marzoli et al.*, 2011; *Merle et al.*, 2011; *Callegaro et al.*, 2013; *Merle et al.*, 2013; *Callegaro et al.*, 2014; *Mazza et al.*, 2014] and arc data from the GEOROC database (http://georoc.mpch-mainz.gwdg.de/georoc/)

Figure 7. Age corrected (200 Ma) Nd-Pb radiogenic isotope comparison between northern, southern and transitional CAMP with data from Paleozoic accreted terranes: Avalonia [*Pe-Piper and Piper*, 1998], Meguma [*Currie et al.*, 1998] and

Carolina [*Pettingill et al.*, 1984; *Sinha et al.*, 1996]. For A-C northern and transitional CAMP plot with the northern accreted terranes, Avalonia and Meguma, while southern CAMP spans all three. Previous workers have shown that crustal contamination cannot account for the isotopic signature of CAMP lavas [*Puffer*, 2001; *Merle et al.*, 2011; *Callegaro et al.*, 2013; *Callegaro et al.*, 2014]. Additional CAMP data can be found in Table S4 [*Dostal and Durning*, 1998; *Marzoli et al.*, 2011; *Callegaro et al.*, 2013; *Merle et al.*, 2013; *Mazza et al.*, 2014]. Radiogenic isotope ratios were age corrected to initial eruptive values at 200 Ma assuming parent/daughter values reported in Tables S1 and S4 and decay constants from *Steiger and Jäger* [1977].

Figure 8. CAMP primary magma compositions on a mole% projection towards diopside into the olivine-quartz-calcium Tschermak's plane after *O'hara*, [1968] with reference values: mantle peridotite (KR-4003) [Walter, 1998], oceanic crust (Siqueiros Fracture Zone) [*Herzberg and Asimow*, 2008], and the composition of subducting sediment (GLOSS-II) from *Plank* [2014]. Most of the CAMP primary magmas plot on the high SiO_2 side of the diagram, possibly indicating a significant silica-rich, olivine-free pyroxenite component in the source. Northern CAMP could not be compared as samples are too evolved to be in olivine control. Additional CAMP data can be found in Table S4.

Figure 9.

Discriminating between metasomatism by fluids or sediment-melt components in CAMP magmas. A) Ba/La-Th/Yb diagram (after [*Woodhead et al.,* 2001]) shows a high Th/Yb trend indicating a sediment-melt component, and a high Ba/La trend indicating a fluid component. Northern and transitional CAMP follow the high Th/Yb trend, while southern CAMP follows the high Ba/La trend. A) CAMP plots similarly to arc magmas on a Dy/Dy*-Dy/Yb diagram (modified from *Davidson et al.* [2013]). Northern and transitional CAMP have higher middle rare earth element MREE contents relative to HREE than southern CAMP as expressed by lower Dy/Dy*. Northern and transitional CAMP show positive trends between Dy/Dy* and Dy/Yb (Fig. 9B). A subset of mostly southern CAMP (including the Virginia basalts samples analyzed for this study) and one northern CAMP sample from the Caraquet dike from New Brunswick [*Dostal and Durning*, 1998] plot in the lower lefthand corner of the diagram (Dy/Dy* < 1.0, Dy/Yb < 1.55). Atlantic MORB averages calculated from from *Janney and Castillo* [2001]. Mantle xenolith data from the GEOROC database (http://georoc.mpch-mainz.gwdg.de/georoc/). Composition of subducting sediment (GLOSS-II) from *Plank* [2014]. As example of possible sediment melt composition we calculated equilibrium melting (at melt fractions 0.05, 0.1, 0.20) starting from GLOSS-II in eclogite facies using the partition coefficients in *Kelemen et al.* [2003].

Figure 10. Schematic model for CAMP formation (not to scale). A) Accretion of Ganderia, Avalonia and Meguma (shown here as one landmass for simplicity)

resulted in metasomatization of the upper mantle beneath Laurentia as well as the formation of pyroxenite through the reaction of slab melts with the overlying peridotite. B) The Alleghanian collisional event begins with oblique collision and flat subduction of the Rheic plate in the North leading to more metasomatism of the mantle wedge and the production of more pyroxenite. The Scranton Rift may have been an indenter to the advancing Gondwanan plate, blocking the advancing thrust sheets. This blockage may have in turn stalled the subduction of the Rheic plate beneath Laurentia. C) The clogging of subduction in the North leads to a rotation of the subduction zone producing head-on collision in the South. This results in metasomatism of the mantle wedge as well as the production of pyroxenite in the South. D) Pangea is formed with the closure of the Rheic ocean. The low angle and stalling of subduction in the North results in the Rheic plate underplating the lithosphere. E) P/T conditions cause the Rheic plate to eclogitize and begin to tear. The plate may have also been weakened by the jamming of the subduction zone. This tear initially leads to small amounts of mantle melting, which form the Coastal New England dike swarm. F) The slab tear propagates in both directions due to slab pull, eventually resulting in a catastrophic delamination event. This delamination produces mantle upwelling (increasing the mantle potential temperature noted as red in the figure), uplift and significant melting of the mantle (CAMP), which had been metasomatized by previous episodes of subduction. Accreted terrane boundaries from *Hibbard et al.* [2010] and *Hatcher* [2010]. Scranton Rift location from *Benoit et al.* [2014]. CAMP boundary after *McHone* [2003]. Scranton Rift location from *Benoit et al.* [2014]. Final closure of Pangea after Hatcher [2002].

Figure 11. Histogram of ages of Late Triassic Coastal New England (CNE) dikes (purple) and plutons (light blue) modified from [*McHone and Butler,* 1984] with updated with ages from [*Pe-Piper and Jansa*, 1986; *Reynolds et al.,* 1987; *Greenough,* 1988; *McHone,* 1992; *Pe-Piper et al.,* 1992; *Sundeen and Huff,* 1992; *Pe-Piper and Reynolds,* 2000; *Ross,* 2010]. The cumulative stratigraphic thickness for the Fundy basin over time [*Schlische et al.,* 2003] is shown as the blue line, which decreases rapidly at the time of CAMP emplacement (indicated by red bar). CNE overlaps with CAMP magmatism in time and uplift may have occurred at the time of CNE emplacement as the majority of CNE coincides with a hiatus in sedimentation in the Fundy basin

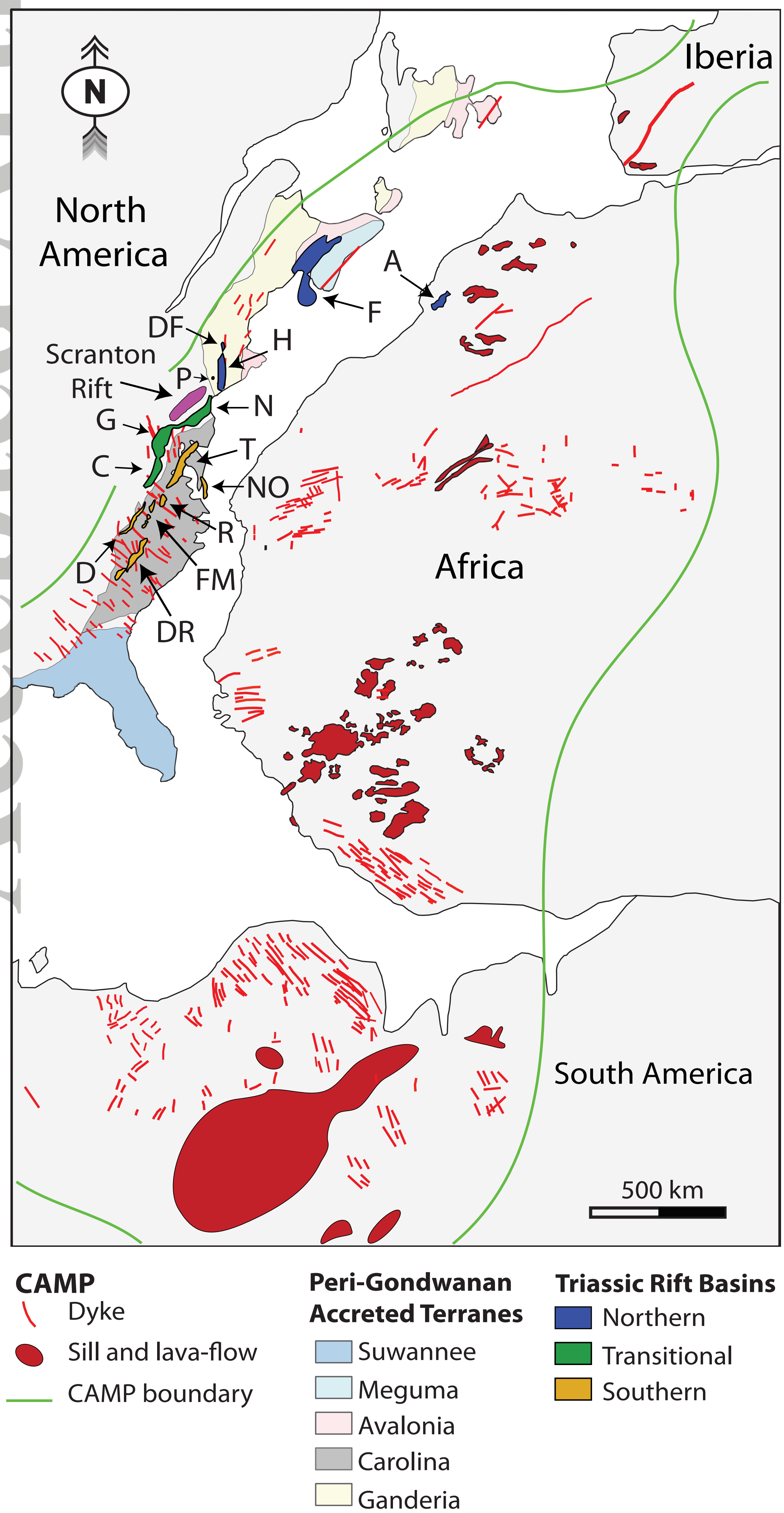
N
North
America
Iberia
A
F
DF
H
Scranton
Rift
P
N
G
T
C
NO
R
D
FM
DR
Africa
South America
500 km
CAMP
Dyke
Sill and lava-flow
CAMP boundary
Peri-Gondwanan
Accreted Terranes
Suwannee
Meguma
Avalonia
Carolina
Ganderia
Triassic Rift Basins
Northern
Transitional
Southern

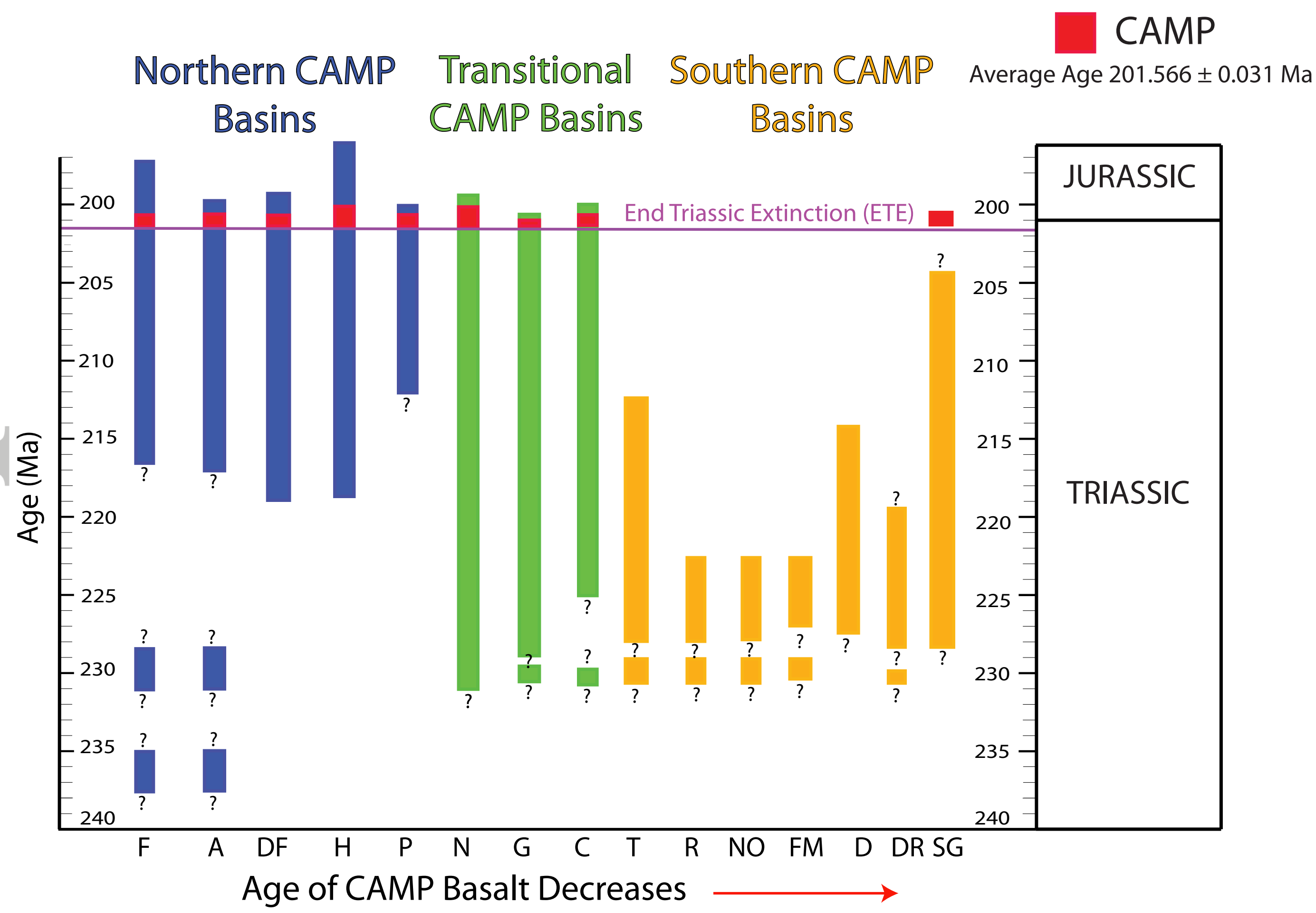
CAMP
Average Age 201.566 ± 0.031 Ma
Northern CAMP Basins
Transitional CAMP Basins
Southern CAMP Basins
End Triassic Extinction (ETE)
JURASSIC
TRIASSIC
Age (Ma)
200
205
210
215
220
225
230
235
240
F A DF H P N G C T R NO FM D DR SG
Age of CAMP Basalt Decreases

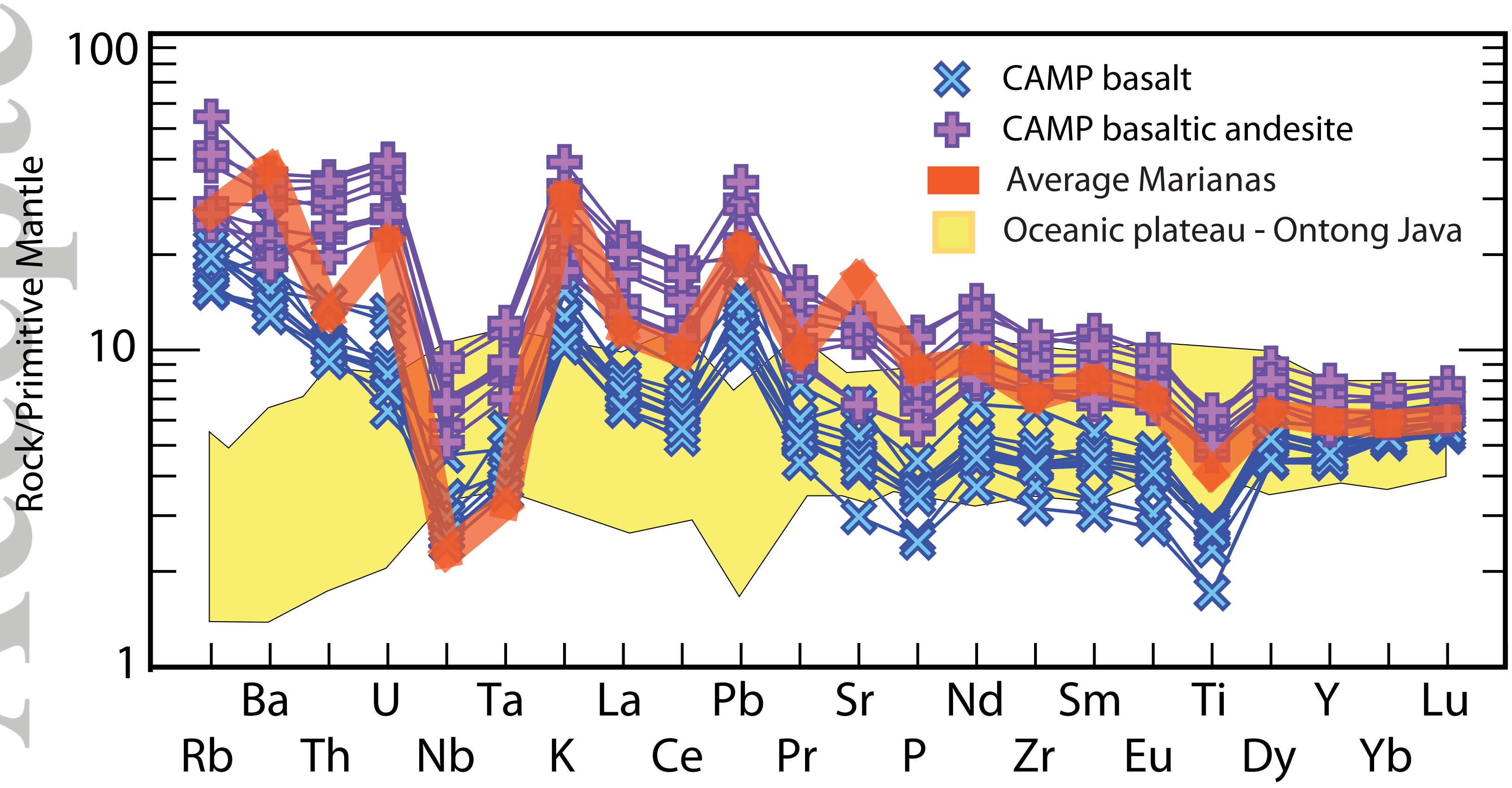
100
10
1
Rock/Primitive Mantle
CAMP basalt
CAMP basaltic andesite
Average Marianas
Oceanic plateau - Ontong Java
Ba
U
Ta
La
Pb
Sr
Nd
Sm
Ti
Y
Lu
Rb
Th
Nb
K
Ce
Pr
P
Zr
Eu
Dy
Yb

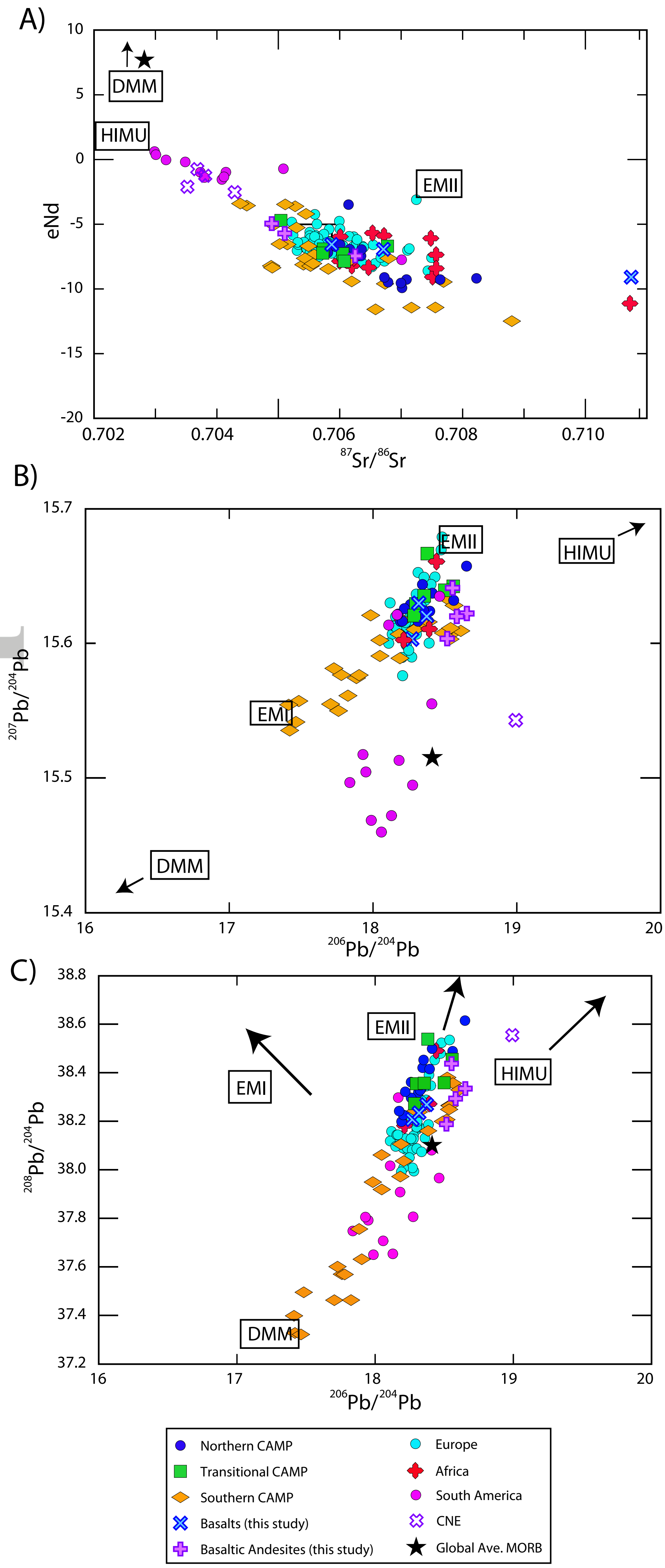
A)
eNd
87Sr/86Sr
DMM
HIMU
EMII
B)
207Pb/204Pb
206Pb/204Pb
EMII
HIMU
EMI
DMM
C)
208Pb/204Pb
206Pb/204Pb
EMII
EMI
HIMU
DMM
Northern CAMP
Transitional CAMP
Southern CAMP
Basalts (this study)
Basaltic Andesites (this study)
Europe
Africa
South America
CNE
Global Ave. MORB

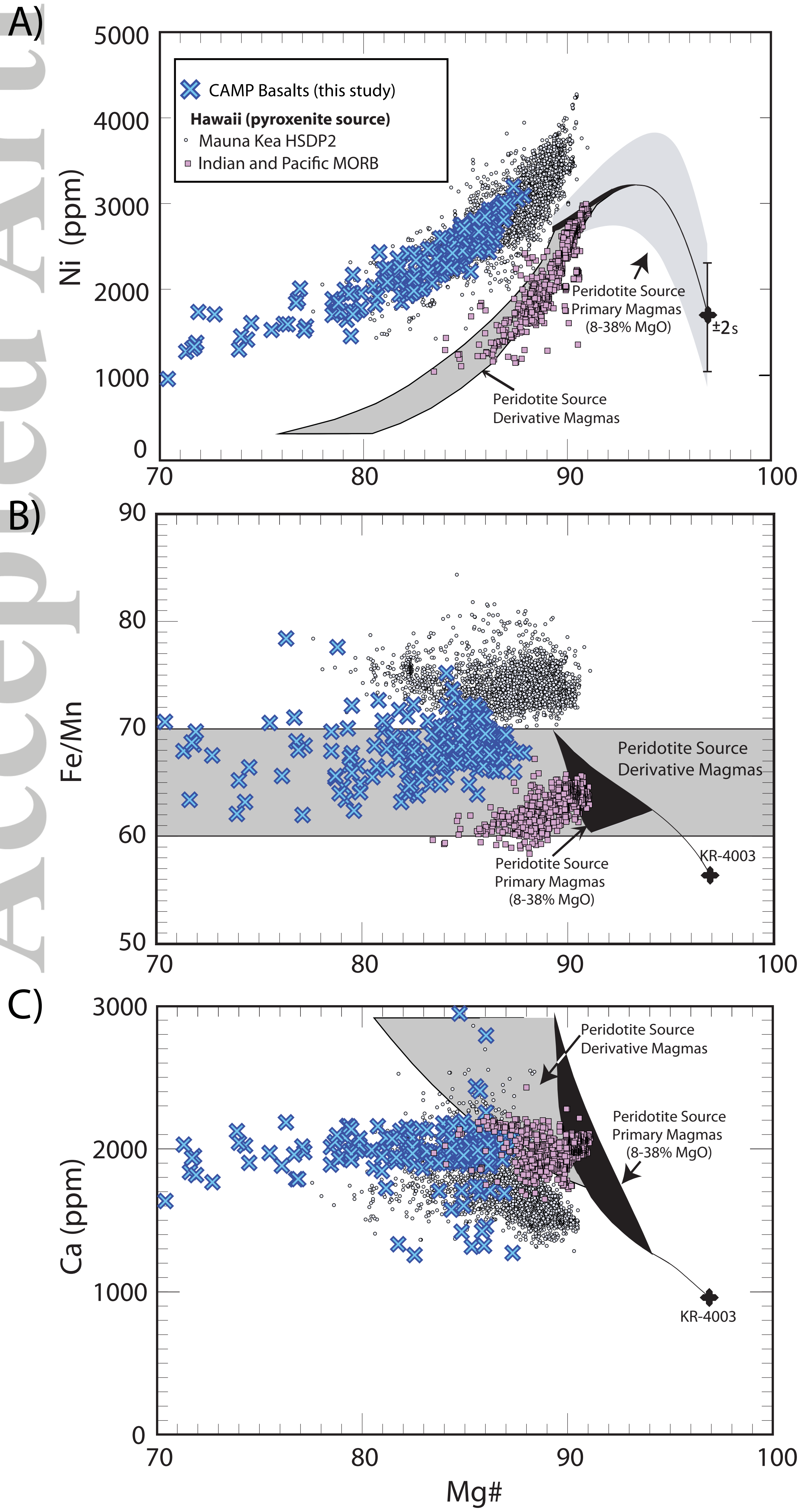
A)
5000
4000
3000
2000
1000
0
Ni (ppm)
CAMP Basalts (this study)
Hawaii (pyroxenite source)
Mauna Kea HSDP2
Indian and Pacific MORB
Peridotite Source
Primary Magmas
(8-38% MgO)
±2s
Peridotite Source
Derivative Magmas
70
80
90
100
B)
90
80
70
60
50
Fe/Mn
Peridotite Source
Derivative Magmas
Peridotite Source
Primary Magmas
(8-38% MgO)
KR-4003
70
80
90
100
C)
3000
2000
1000
0
Ca (ppm)
Peridotite Source
Derivative Magmas
Peridotite Source
Primary Magmas
(8-38% MgO)
KR-4003
70
80
90
100
Mg#

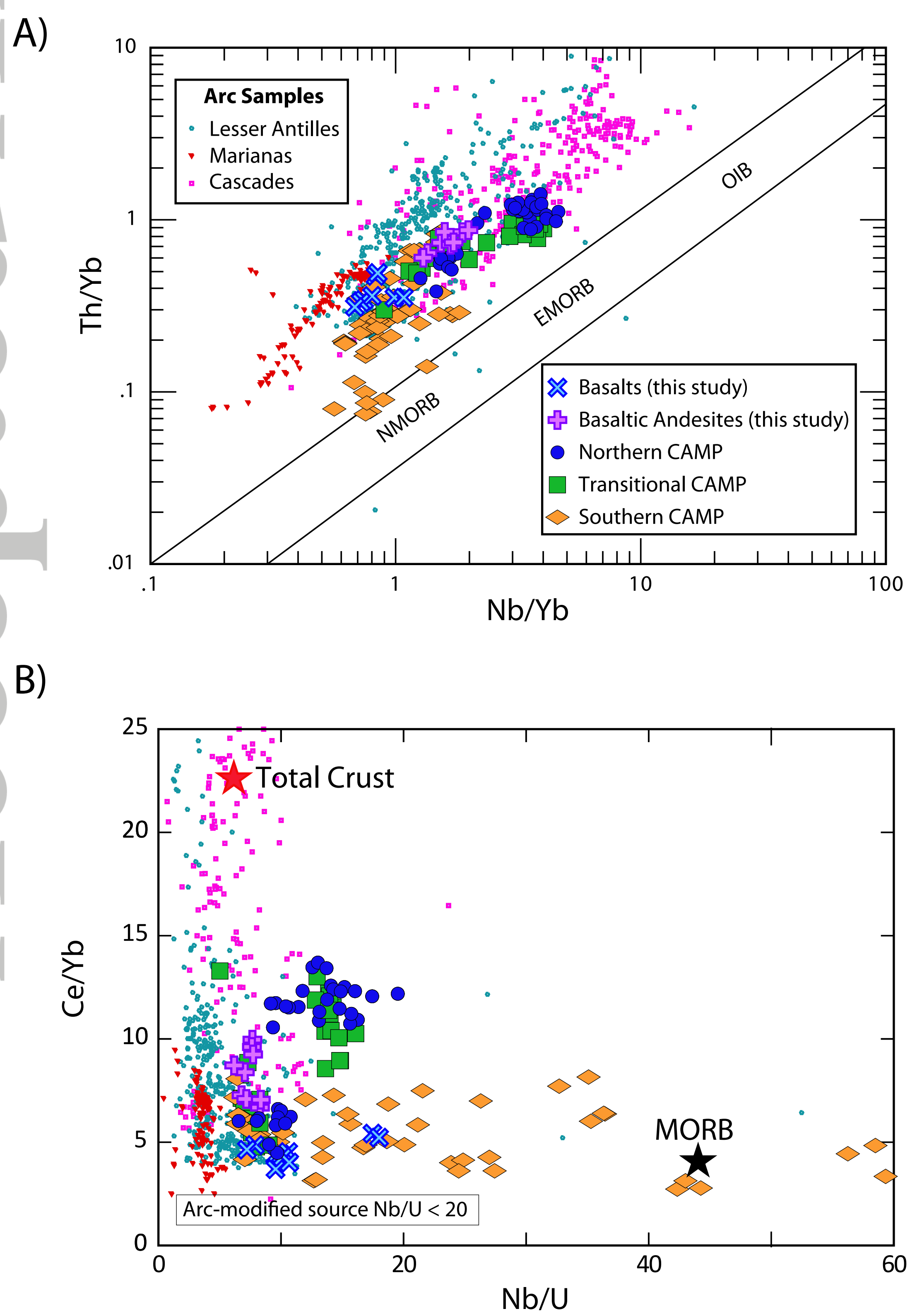
A)
Arc Samples
Lesser Antilles
Marianas
Cascades
Th/Yb
Nb/Yb
OIB
EMORB
NMORB
Basalts (this study)
Basaltic Andesites (this study)
Northern CAMP
Transitional CAMP
Southern CAMP
B)
Ce/Yb
Nb/U
Total Crust
MORB
Arc-modified source Nb/U < 20

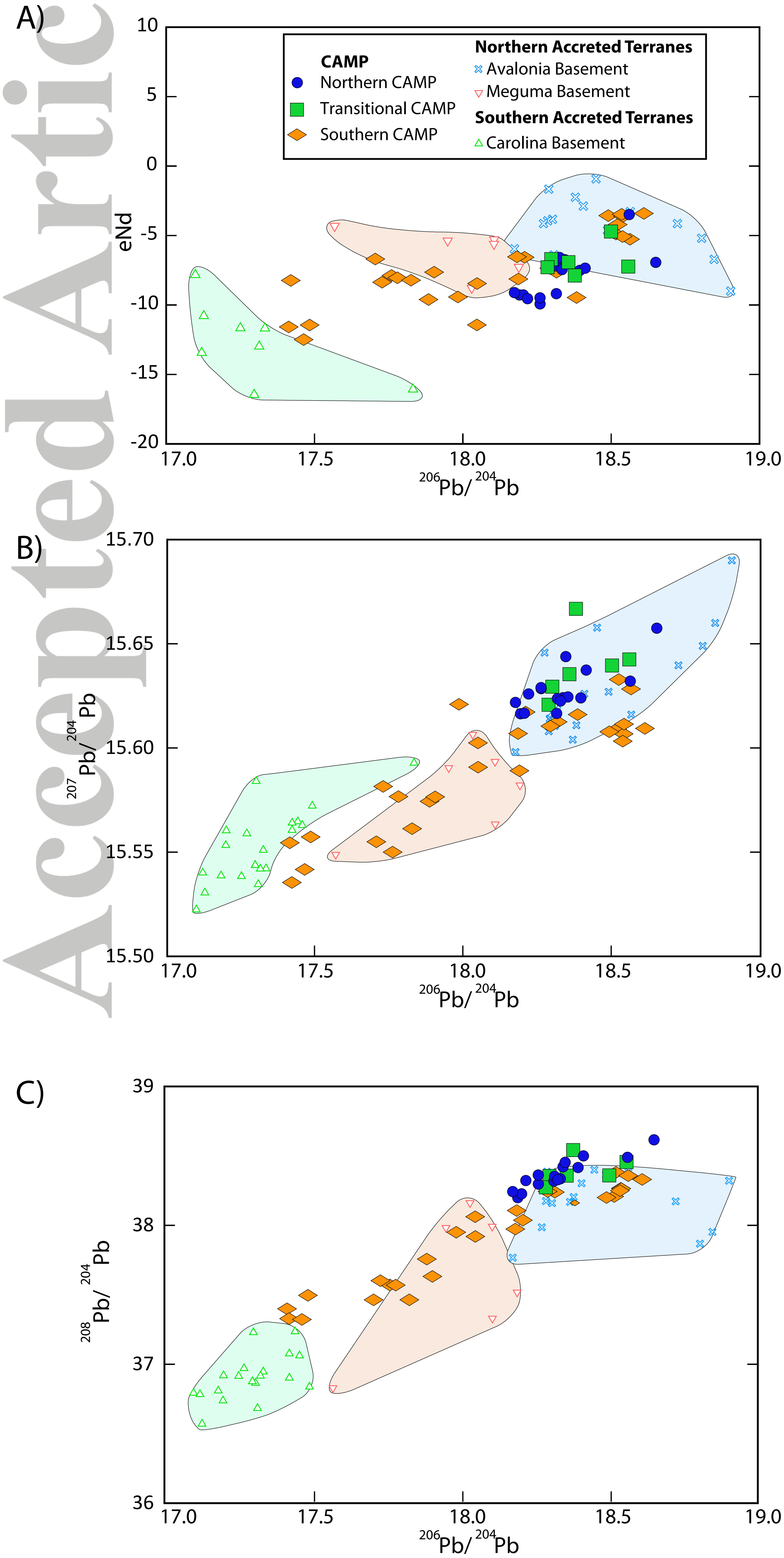
A)
CAMP
Northern CAMP
Transitional CAMP
Southern CAMP
Northern Accreted Terranes
Avalonia Basement
Meguma Basement
Southern Accreted Terranes
Carolina Basement
eNd
206Pb/204Pb
B)
207Pb/204Pb
206Pb/204Pb
C)
208Pb/204Pb
206Pb/204Pb

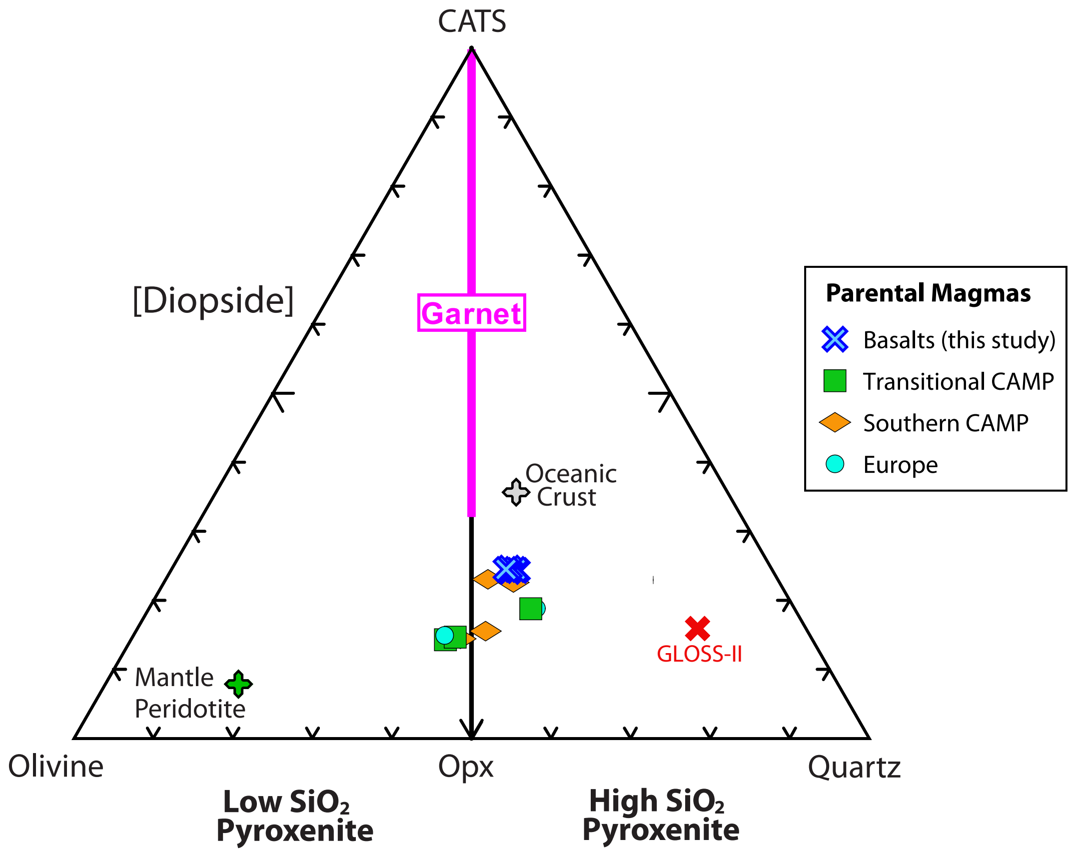
CATS
[Diopside]
Garnet
Oceanic
Crust
Mantle
Peridotite
GLOSS-II
Olivine
Opx
Quartz
Low SiO_2
Pyroxenite
High SiO_2
Pyroxenite
Parental Magmas
Basalts (this study)
Transitional CAMP
Southern CAMP
Europe

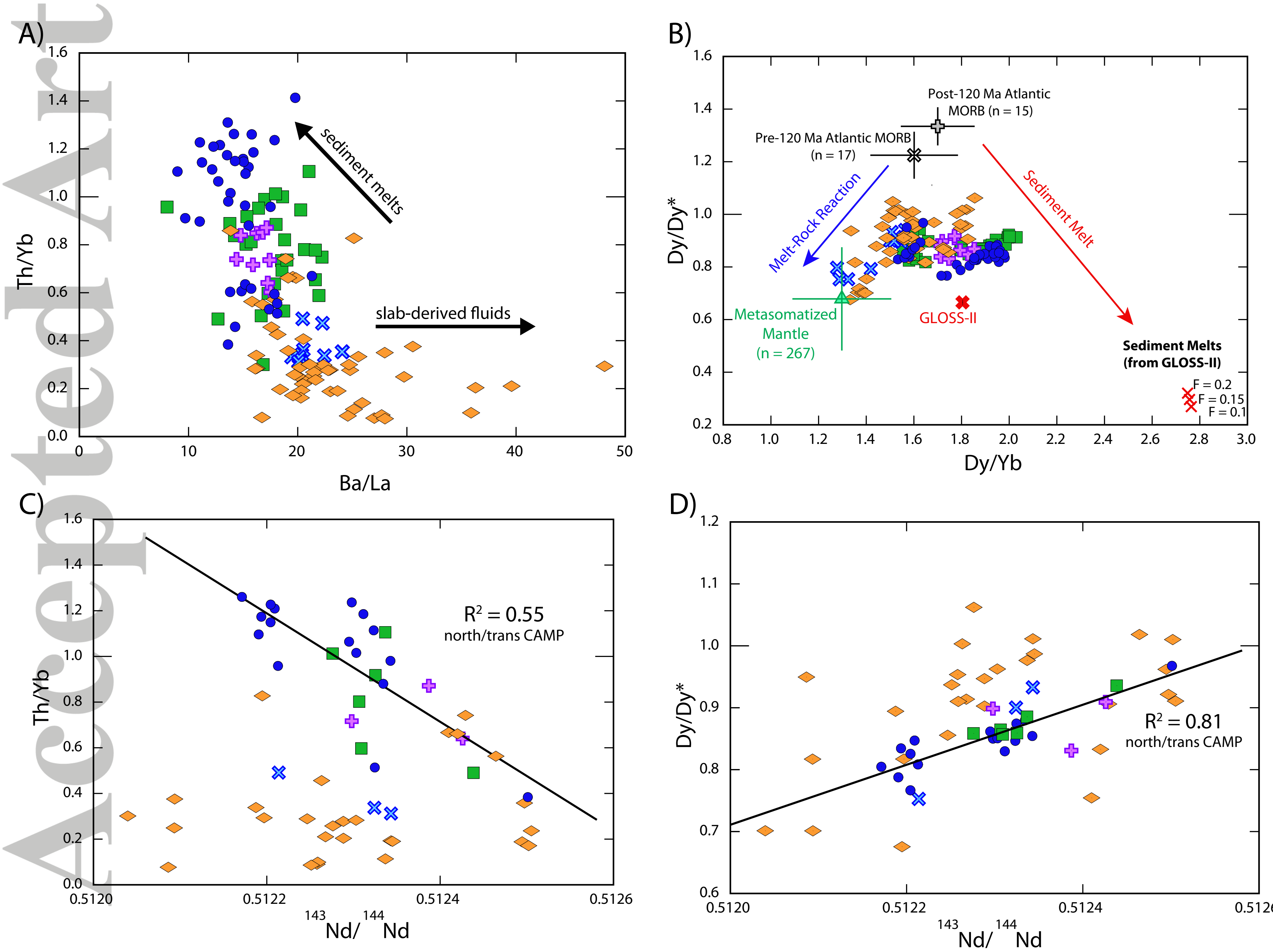
A)
Th/Yb
Ba/La
sediment melts
slab-derived fluids
B)
Dy/Dy*
Dy/Yb
Post-120 Ma Atlantic MORB (n = 15)
Pre-120 Ma Atlantic MORB (n = 17)
Melt-Rock Reaction
Sediment Melt
Metasomatized Mantle (n = 267)
GLOSS-II
Sediment Melts (from GLOSS-II)
F = 0.2
F = 0.15
F = 0.1
C)
Th/Yb
R² = 0.55
north/trans CAMP
143Nd/144Nd
D)
Dy/Dy*
R² = 0.81
north/trans CAMP
143Nd/144Nd

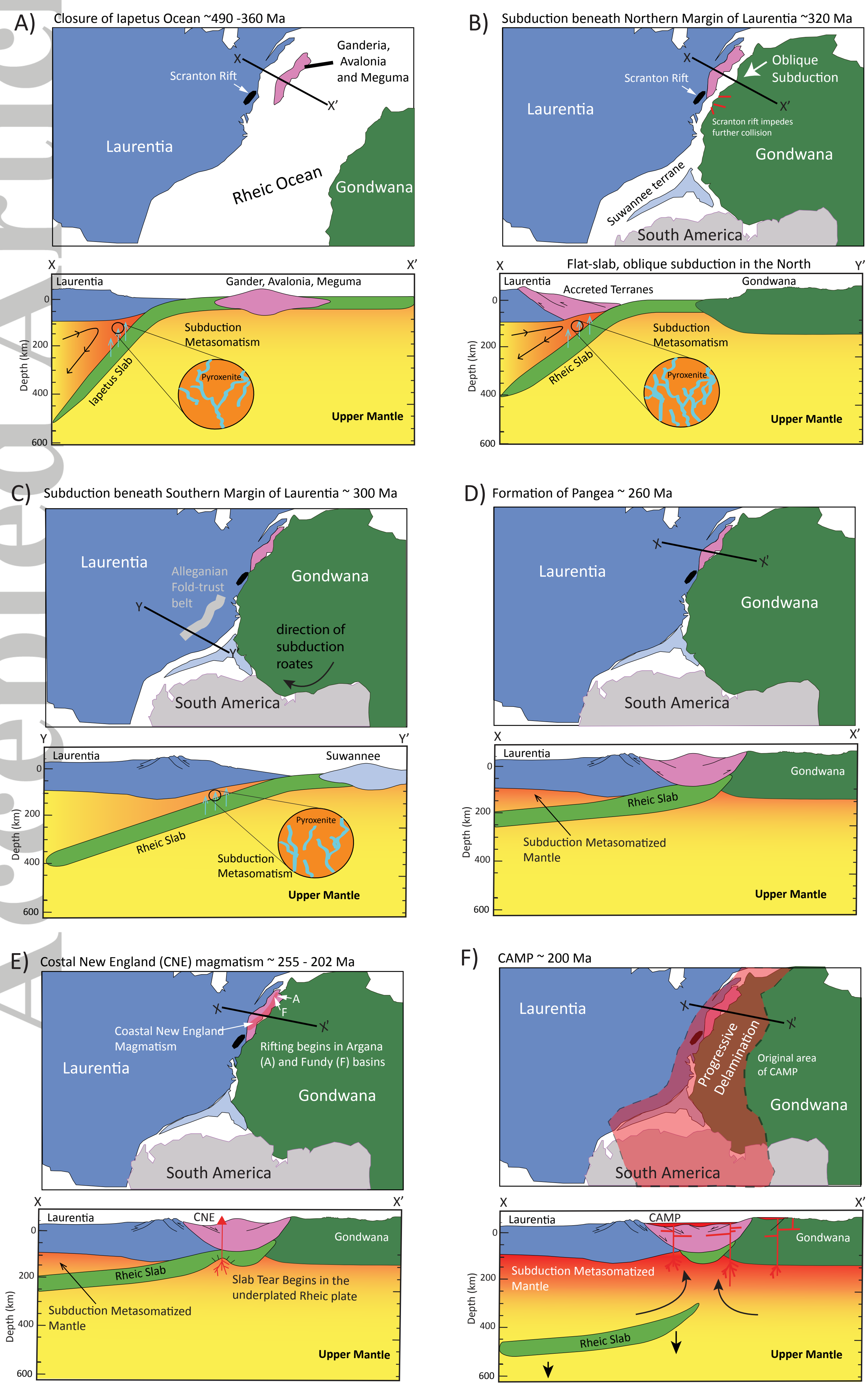
A)
Closure of Iapetus Ocean ~490 -360 Ma
Ganderia, Avalonia and Meguma
Scranton Rift
X
X'
Laurentia
Rheic Ocean
Gondwana
Laurentia
Gander, Avalonia, Meguma
Subduction Metasomatism
Pyroxenite
Iapetus Slab
Upper Mantle
Depth (km)
0
200
400
600
B)
Subduction beneath Northern Margin of Laurentia ~320 Ma
Oblique Subduction
Scranton Rift
Laurentia
Scranton rift impedes further collision
Gondwana
Suwannee terrane
South America
Flat-slab, oblique subduction in the North
Laurentia
Accreted Terranes
Gondwana
Subduction Metasomatism
Rheic Slab
Pyroxenite
Upper Mantle
C)
Subduction beneath Southern Margin of Laurentia ~ 300 Ma
Laurentia
Alleganian Fold-trust belt
Gondwana
Y
Y'
direction of subduction roates
South America
Laurentia
Suwannee
Pyroxenite
Rheic Slab
Subduction Metasomatism
Upper Mantle
D)
Formation of Pangea ~ 260 Ma
Laurentia
Gondwana
South America
Laurentia
Gondwana
Rheic Slab
Subduction Metasomatized Mantle
Upper Mantle
E)
Costal New England (CNE) magmatism ~ 255 - 202 Ma
A
F
Coastal New England Magmatism
Laurentia
Rifting begins in Argana (A) and Fundy (F) basins
Gondwana
South America
Laurentia
CNE
Gondwana
Rheic Slab
Slab Tear Begins in the underplated Rheic plate
Subduction Metasomatized Mantle
Upper Mantle
F)
CAMP ~ 200 Ma
Laurentia
Progressive Delamination
Original area of CAMP
Gondwana
South America
Laurentia
CAMP
Gondwana
Subduction Metasomatized Mantle
Rheic Slab
Upper Mantle

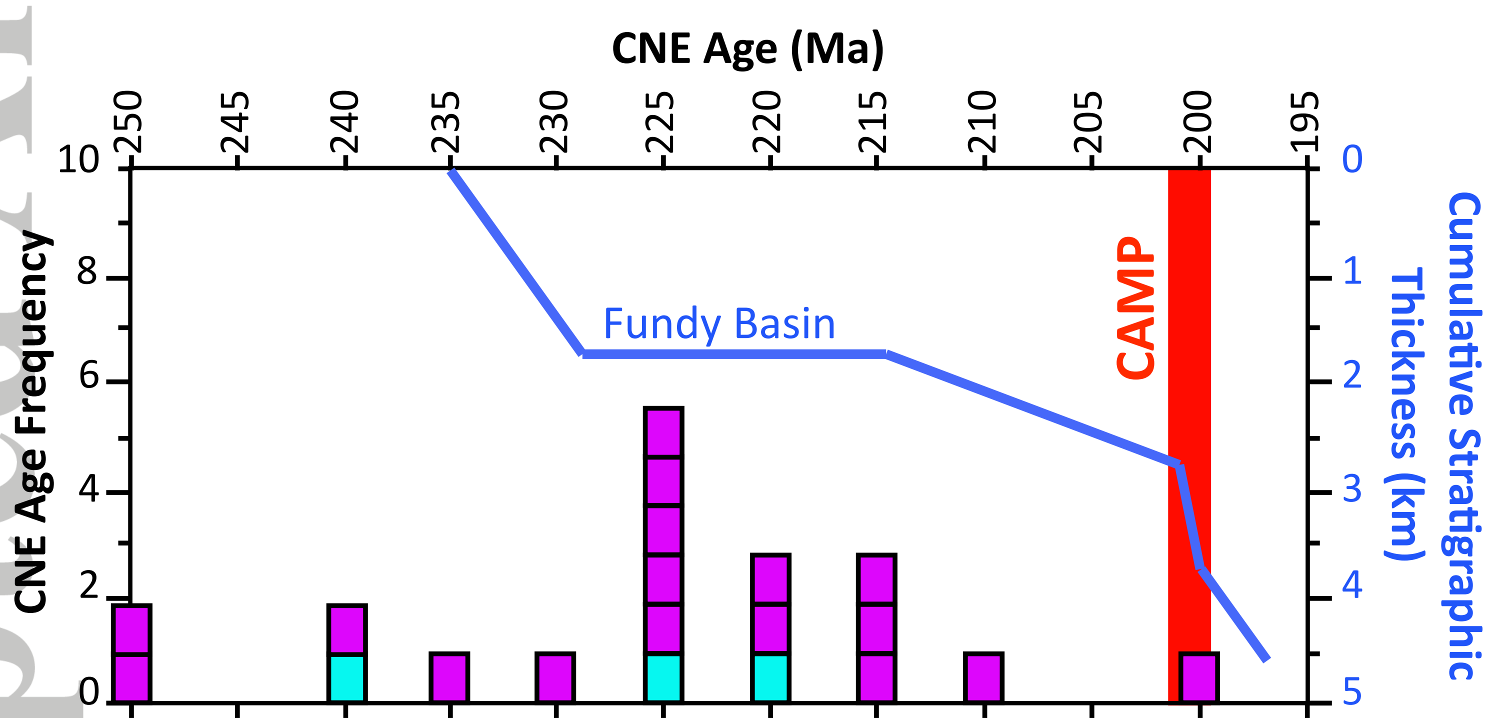
CNE Age (Ma)
250 245 240 235 230 225 220 215 210 205 200 195
CNE Age Frequency
10 8 6 4 2 0
Cumulative Stratigraphic Thickness (km)
0 1 2 3 4 5
Fundy Basin
CAMP